
# Recent developments in the catalytic conversion of syngas to SAF

E.H. Boymans, Y. Ganjkhanlou, I. Aguirrezabal, N. Viar

This project has received funding from the European Union's Horizon Europe research and innovation programme under grant agreement No.

Table 1: Document information

| Document Information | |
|---|---|
| Project name: | ICARUS |
| Project title: | International Cooperation for sustainable aviation biofuels |
| Project number: | 101122303 |
| Start date: | 01-10-2023 |
| Duration: | 3 years |
| Dissemination level | Public |

| Version history | Date | Version | Name |
|---|---|---|---|
| Document created | 14-03-2024 | V1 (merged chapters and reviewed) | Evert Boymans (TNO) |
| Reviewed | 22-03-2024 | V1 | Yadi Ganjkhanlou (TNO) |
| | 25-03-2024 | V2 | I. Aguirrezabal, N. Viar (EHU) |
| | | | |
| | | | |

ACKNOWLEDGMENT & DISCLAIMER

This project has received funding from the European Union's Horizon Europe research and innovation programme under grant agreement No 101122303.

## Table of Contents

# 1 Introduction

In the ICARUS project, three sustainable aviation fuel (SAF) production routes have been selected in which further technology development can result in wider deployment. In the project, the entire value chains are considered, including techno-economic, environmental, and social assessments. The standard regulating the technical certification of synthetic aviation fuel and sustainable aviation fuel is described in ASTM D7566 and can be found in Table 2.[1] Each process has its own maximum blending ratio that can be used in combination with conventionally (fossil-based) jet fuel specified in ASTM standard D1655. In ICARUS, technological improvements for the three routes were considered including (HTL) bio-oils-to-SAF, isobutanol-to-SAF and biosyngas-to-SAF.

This work, as part of Task 1.4, will include a literature survey to identify state-of-the-art catalysts for the conversion of syngas into SAF. First the commercial FTS benchmark will be described in a chapter, followed by the novel alternative routes with the accompanied references. These latter routes are separated in different chapters as

- **Direct syngas-to-jet**, (Chapter 3) an integrated FT-based catalyst design to deviate from the ASF distribution and produce jet fuel in one step.
- **Syngas-to-olefins(-to-jet).** (Chapter 4) a more alternative pathway with a potentially higher carbon selectivity to SAF compared to traditional FTS. The required oligomerization and hydrogenation to produce jet-grade SAF will also be considered.
- **Syngas-to-alcohols(-to-jet).** (Chapter 5) Alcohol pathway, followed by a brief description of consecutive steps.

The objective is to identify catalysts and/or reactor technology enabling a more selective syngas-to-SAF process with +50% carbon selectivity compared to the commercial FTS benchmark of 40-45%. Additional potential benefits include that the complex refining will be simplified while reducing costs as e.g., wax formation and separation will be avoided. The most important selection criteria will be the (estimated) carbon selectivity of the entire process from syngas to SAF based on the reported values of state-of-the-art. Other criteria will include the total conversion units needed to obtain SAF, the viability of the catalyst production and the quality of the product fuel. With this, a syngas conversion route will be selected for further development to TRL-5 that will eventually result in a wider deployment of the syngas-to-SAF process.

*Table 2: Overview of the ASTM D7566-23b annexes describing the different (biobased) processing routes.*

| Annex | Title | Product name | Manufacture | Max. Blending |
|---|---|---|---|---|
| A1 | Fischer-tropsch hydroprocessed synthesized paraffinic kerosine | FT-SPK | Fischer-Tropsch (FT) process using Iron or Cobalt catalyst with subsequent hydroprocessing. | 50% |
| A2 | Synthesized paraffinic kerosine from hydroprocessed esters and fatty acids | HEFA SPK | Hydrogenation and deoxy-genation of fatty acid esters and free fatty acids with subsequent hydroprocessing. | 50% |
| A3 | Synthesized iso-paraffins from hydroprocessed fermented sugars | SIP | Hydroprocessed synthesized iso-paraffins wholly derived from farnesene produced from fermentable sugars with subsequent hydroprocessing. | 10% |
| A4 | Synthesized kerosine with aromatics derived by alkylation of light aromatics from non-petroleum sources | SPK/A | FT SPK as defined in Annex A1 combined with synthesized aromatics from the alkylation of non-petroleum derived light aromatics (primarily benzene) with subsequent hydroprocessing. | 50% |
| A5 | Alcohol-to-jet synthetic paraffinic kerosene (atj-spk) | ATJ-SPK | Synthesized paraffinic kerosene wholly derived from either ethanol or isobutanol through oligomerization, hydrogenation, and fractionation. | 50% |
| A6 | Synthesized kerosine from hydrothermal conversion of fatty acid esters and fatty acids | CHJ (Catalytic Hydrothermolysis Jet) | Hydrothermal conversion of fatty acid esters and free fatty acids with subsequent hydroprocessing. | 50% |
| A7 | Synthesized paraffinic kerosine from hydroprocessed hydrocarbons, esters and fatty acids | HC-HEFA SPK | Paraffins derived from hydrogenation and deoxy-genation of bio-derived hydrocarbons (Botryococcus braunii species of algae), fatty acid esters, and free fatty acids. | 10% |
| A8 | Alcohol-to-jet synthetic paraffinic kerosene with aromatics (atj-ska) | ATJ-SKA | Addition to ATJ-SPK of an aromatic product stream comprising dehydration, aromatization, hydrogenation, and fractionation. | 50% |

# 2 Commercial SAF production

## 2.1 Fischer-Tropsch to Jet

The reactions relevant for the Fischer-Tropsch synthesis (FT or FTS) are shown below.

Reactions of interest:

| | | | | |
|---|---|---|---|---|
| FTS: | $CO + 2\ H_2$ | ⇆ | $-CH_2- + H_2O$ | ($\Delta H_r^0$ = -165 kJ/mol) |
| WGS: | $CO + H_2O$ | ⇆ | $H_2 + CO_2$ | ($\Delta H_r^0$ = - 41 kJ/mol) |
| $CH_4$ | CO + 3 H2 | ⇆ | $CH_4 + H_2O$ | ($\Delta H_r^0$ = -206 kJ/mol) |

Fe, Co, Ni and Ru are active in the FTS, but only the former two are used commercially. Their activity decreases as follows: Fe > Co > Ni > Ru when there is no support.[2] In contrast, the use of alumina support for each active metal markedly influences the activity as follows: Ru > Fe > Ni > Co. It should be mentioned that Ru catalysts are less desirable because of their high cost and low availability. Ni is susceptible to coke formation and it has a high methane selectivity. Therefore, Co and Fe are the preferred catalysts for the FT synthesis.[2] Iron-based catalysts for FTS offer distinct advantages like affordability, sulfur tolerance, and operational flexibility, making them attractive for industrial use. However, compared to cobalt-based catalysts, they exhibit lower activity at low/medium temperatures, are less selective to jet fuel range hydrocarbons and more selective to olefins, $CO_2$ and other oxygenates. Conversely, cobalt catalysts favor long-chain hydrocarbons while minimizing the water-gas shift (WGS) reaction. The performance of these catalysts can be improved by changing their properties including particle size, dispersion, crystalline phases, additives, promoters, and support materials. Other process parameters such as temperature, pressure, feed gas composition and reactor configurations (for efficient mass and heat transfer) also affect the FTS efficiency and selectivity.[3,4]

By carefully optimizing these factors, the selectivity towards methane and $CO_2$ can be lowered ultimately directing the process towards the desired production of $C_{5+}$ hydrocarbons. The precise mechanism remains an ongoing discussion within the scientific community. Despite this, the following key steps are suggested as the main reaction sequence:

1. Adsorption and Dissociation: CO and $H_2$ adsorb and dissociate on the catalyst surface.
2. Surface Intermediates: Various CHx species (x = 0-3) form on the surface.
3. Chain Growth and Termination: C-C bond formation through coupling CHx species, leading to surface CnHm intermediates (n ≥ 2). Alternatively, hydrogenation of CHx species to methane.
4. Product Formation: Dehydrogenation or hydrogenation of CnHm intermediates yields olefinic or paraffinic products.

Conventional FT catalysts adhere to the Anderson-Schulz-Flory (ASF) law[5,3] (equation 1), limiting selectivities to specific hydrocarbon fractions. The ASF model explains that the molar fraction ($M_n$) of the product with a carbon number of n is only dependent on the chain growth probability (α), which is a function of the chain growth and chain termination rates, by the following equation:

$$M_n=(1-\alpha)\alpha^{n-1} \quad (1)$$

## Commercial FT plants

The Fischer-Tropsch technology applied commercially can be divided into high temperature Fischer-Tropsch (HTFT) in 2-phase operation at ca. 320-350 °C and low temperature Fischer-Tropsch (LTFT) at ca. 200-250 °C in 3-phase operation.[6]

For the HTFT operation, all the formed products remain in the gas phase allowing the application of circulating or fixed fluidized bed reactors. Iron is applied as catalyst, because cobalt would lead to primarily methane formation at the high temperature. Lower hydrocarbons, C1-C10, are mostly obtained from this HTFT process which are suitable for gasoline production of which linear 1-olefins and some oxygenates can be obtained as chemical precursors.

In LTFT operation, liquid products including heavy paraffins up to C22+ are formed next to gaseous products in the reactor. Due to the presence of liquids, fluidized beds cannot be used and either wall-cooled fixed bed or slurry bed reactors are chosen. Cobalt is applied mostly in LTFT operation, because of its high lifetime, stability and the possibility to reach high conversions per pass. These advantages outweigh the much higher price of cobalt compared to iron.[7] According to the Shell Middle Distillate process (SMDS) the mostly paraffinic C5+ products are then converted through hydrotreatment into a middle distillate with a boiling point of ca. 150-360 °C (ca. C11-C20) and some naptha[1].[8] Hydrotreatment here includes the hydrocracking of the heaviest hydrocarbons in combination with hydroisomerization, preferably under "ideal hydrocracking" conditions implying that the biggest molecules reactor first thereby preventing overcracking.[9]

The SMDS approach forms the basis of the Shell Bintulu plant that started operating in 1992 with a capacity of 14,500 bpd. Also, the much larger Pearl GTL plant with a plant capacity of 140,000 is based on this SMDS approach. However, in the Pearl GTL plant, also paraffin waxes and lubricant oils are obtained as by-products.[10]

An overview of the commercial FT plants can be found in review paper by Gholami et al..[11] The required syngas is produced from fossil feedstocks, historically coal, but currently mostly natural gas. Shell's Bintulu SMDS and Pearl GTL plants make use of the multitubular fixed bed LTFT approach. Sasol also has several production facilities dating back to 1955 applying HTFT as well as LTFT. Sasol's largest Secunda plant, the largest single emitter of GHGs in the world as a coal liquefaction plant, operates under HTFT conditions.[12] Whereas their most recent ORYX GTL plant in Qatar is operational since 2007 also applies LTFT but in slurry phase reactors.

Fischer-Tropsch-Synthesis in a microstructured reactor has been described already more than 10 year ago[13], and a first technical application has been presented in 2011 by the company Velocys.[14] This in combination with a unique catalyst from Oxford catalysis. This technology exhibits significantly better performance in term of catalyst productivity with over 80% CO conversion per pass. Similarly INERATEC GmbH, a spin-off from KIT, has developed and commercialized microreactors with a focus on carbon-neutral liquid fuels production and Power-to-X. It has been able to scale up its microreactors more than 5,000 times from their lab-scale setup to reactors that can produce up to 2 BPD hydrocarbon product. The zigzag shaped channels showed much higher conversion rates than the conventional straight microchannels.[15]

These commercial processes, and the microchannel technology are developed for liquid synthesis and not specifically SAF and the dominant design factor in reactor technology is based on the FTS heat management. The selectivities to specific fuels are tailored based on the refinery approaches, if the syncrude is not already perceived as the main product for further (co-)processing. In other words, no specific catalysts are used that deviate strongly from the ASF distribution in one conversion step. In

[1] "Jet fuel, diesel fuel, and the lighter grades of fuel oil are collectively referred to as middle distillate fuels, from the fact that they are taken off the middle of a distillation column, below the light ends, such as gasoline and naphtha, and above the heavy ends and resids." Diesel bp 150-380 °C, in Sie they state diesel=gas oil at 250-360 °C. But kerosene stated 150-250 °C, which is too low for Jet!!

the next chapter, the maximum selectivities that can be achieved using LTFT will be explained, leaving room for optimization in ICARUS.

## Selectivity towards SAF production

Production of Jet fuel from syngas through FT synthesis is described in ASTM D7566.[1] Specifically in Annex A1 "Fischer-tropsch hydroprocessed synthesized paraffinic kerosine (SPK)", with no aromatic content (max. 0.5 wt%) as expected from the Co-LTFT approach. In Annex A4 "Synthesized kerosine with aromatics derived by alkylation", aromatics are also considered as part of the fuel at max. 20 vol%. This aromatic fraction is obtained through the alkylation of light aromatics. The aromatics are non-petroleum based and the olefins used for alkylation are produced in FT.

Selected properties for Jet A-1 and the carbon range definition that will be assumed in this work can be found in Table 3. It is important to note that the upper limit for the hydrocarbon range is restricted by the maximum boiling point, whereas the lower limit is indirectly set by the density and viscosity specifications. Another important specification is the low freezing point which dictates a certain degree of branching of the saturated hydrocarbons. Even though, a C10-C18 (branched) hydrocarbon range would fit better in terms of individual boiling points, in this work we will assume a C8-C16 carbon range for comparison reasons.

*Table 3: Selected properties of Jet A-1 turbine aviation fuel as defined by ASTM D1655.*

| Property | | Min | Max |
|---|---|---|---|
| Boiling range | [°C] | 205 (10%) | 300 |
| Density at 15 °C | [kg/m3] | 775 | 840 |
| Freezing point | [°C] | | -40 (Jet A) -47 (Jet A-1) |
| Viscosity -20 °C | [mm2/s] | | 8.0 |
| | | | |
| Carbon range (isomerized) | | C8 | C16 |

One of the refinery approaches to obtain jet fuel from Co-LTFT is the SMDS process.[8] Refining here involves hydrotreatment of the liquid C5+ which isomerises and cracks the waxes to produce mostly liquids. This approach can affort a high yield of jet fuel, as the production of lights is limited and the heaviest fraction get hydrocracked into the desired range. Co-LTFT followed by a hydrotreatment tailored for jet fuel production can provide a 25/50/25 naphtha/kerosene/diesel ratio.[8] At a 90% C5+ selectivity this would provide **45% selectivity** hydrocarbons in the jet fuel range.

A range of products from a SMDS process is naturally not an issue if all products can be used in different applications. However, especially for smaller installations e.g. with biobased feedstocks, it might be desirable to produce predominantly jet fuel range hydrocarbons.[16] With a refinery tailored to maximize jet fuel production, a higher yield could be obtained. In such alternative refinery approach as presented by the Klerk[17], not the complete C5+ liquid stream is combined and hydrotreatment, but only the C9+ is hydrocracked. The more volatile C6-C8 fraction could also be upgraded partially to Jet fuel through aromatisation and the lower olefins can be oligomerized. In this approach, a selectivity of 63 % can be obtained, which is higher than the roughly 50 % obtained with the SMDS approach. However, it can be seen that a tailored jet fuel refinery will become a much more complex and costly plant with an additional three conversion steps. Each conversion requires additional catalysts and most require pure hydrogen gas, which adds additional OPEX to the process.

It is also noteworthy that the selectivity is based on the carbon selectivity from CO. However, in a thermochemical conversion of a biobased feedstock, also much carbon is present in the form of carbon dioxide, $CO_2$ which is not converted in Co-LTFT.

An overview of the obtained carbon selectivities for the different approaches can be found in Table 4, including the SMDS approach and the hypothetical high-Jet approach. It also includes an estimation of the amount of conversion units, including FTS, that would be required, excluding phase separations or distillation which will be required in all processes.

As seen, in order to improve upon the state-of-the-art, the aim will be to achieve a jet fuel (C8-C16 range) selectivity of at least 50%, at the minimum required conversion units.

*Table 4: Carbon selectivity to Jet fuel and required conversion steps in different refinery approaches.*

| Process | Strategy | Jet fuel selectivity (from syngas) % | Conversion units[a] |
|---|---|---|---|
| SMDS | LTFT + HT | 45 | 2 |
| Jet fuel specific | LTFT + HT<br>+ Oli<br>+ Ar | 63 | 4 |

a) Phase separations or distillation not included.

## 2.2 Alcohols to Jet (ATJ)

### 2.2.1 Conventional fermentation-based ATJ

Among the available alcohols for SAF production via alcohol-to-jet (ATJ) pathways, ethanol, n-butanol, and iso-butanol stand out given their easier production via fermentative steps. Such processes seem straightforward when using sugar from edible plants, as it´s known process in food-industries, for instance. Carbohydrate fermentation from biomass that is not considered edible (such as lignocellulose) or nonconventional C-sources, however, requires more sophisticated reaction or separation units, often involving modified yeasts.

When ATJ upgrading steps proceed via alcohol dehydration and olefin oligomerization into SAF-range hydrocarbons, higher alcohols theoretically obtain higher yields even when the maximum carbon yield may be identical. As dehydration proceeds through the removal of hydroxyl groups to form water and thus a loss of mass, a O-based reduction yield is higher for larger alcohols. In addition, this is attributed to oligomerization events with less steps as required for larger olefin reactants, allowing better control over desired product selectivity. This, in turn, results in process costs that are lower for oligomerization units. In contrast, lighter alcohols may lead to C-numbers in the final SAF mixture with a more even distribution, yielding smoother distillation curves. The SAF production intends to resemble petrol-based jet-fuel, and thus the oligomerization steps aim to mimic such mixtures avoiding oligomerization events into too short ($C_4$-$C_8$) or too long ($C_{16+}$) hydrocarbons from $C_2$-$C_4$ olefins.[18]

The dehydration of alcohols through catalytic means has been predominantly been a way to produce relevant chemicals such as ethylene from ethanol, as a substitute of pretrochemically derived olefin sources. Such dehydration has been thoroughly studied under lab-scale and industrial conditions using catalysts with surface acid-features, such as zeotypes, silicoaluminumphosphates, and heteropolyacids.[19] The specific ethanol-to-ethylene step has been commercialized by Syndol using active and selective $Al_2O_3$–$MgO/SiO_2$ heterogeneous catalysts.[20] Given to the minor commercially availability of larger alcohols, and even when dehydration chemistry proceeds though analogous reaction pathways and acid-catalysts, the dehydration of C4 alcohols is less explored. The reactivity of C4 olefins (1/2-butene or isobutene) is expected to be higher given their larger affinity to accept protons from acid-catalysts such as zeolites, and thus isobutanol can lead a pool of C4 isomers or even easily trigger oligomerization reactions.

A critical parameter in dehydration catalysts is the tolerance to large amounts of water, and specifically steam under the operated temperatures and pressures. This is especially critical for oligomerization catalysts involving aluminosilicates[21], and thus they require water-removal steps prior to oligomerization reactors. Depending on the content of water under operated temperature and pressure conditions, such water removal may require to combine distillation, liquid-liquid extraction or adsorption steps to remove water. Unreacted alcohols are also recycled and mixed with the feeding prior to the alcohols and water separation that occurs when such streams are originated from fermentative process.

Light olefin oligomerization steps are well-established in the petrochemical field. The ATJ route requires to reach sufficiently large hydrocarbons ($C_8$-$C_{16}$) to meet the standards in jet-fuel industry. This implies the use of catalysts and reaction conditions (temperature, pressure and reactant contact time) that controls oligomerization with adequate chain-growth probability into desired hydrocarbon range and fuel specifications. For such reason, the design of oligomerization reactors may need to be adapted to the starting alcohol and thus the resulting olefin size. Commercial examples exist for ethylene oligomerization as for the one-step Chevron-Phillips Ziegler, other two-steps or the SHOP process from Shell. Ethylene oligomerization units in ATJ preferentially produce C10 and C12 olefins, indicative of 4-5 oligomerization events.[22] The C4 olefin oligomerization, however, requires less oligomerization events (n=2-3) to reach desired C12-C16 range using un-saturated acid-catalysts such as Amberlyst.[23] The combination of acid-catalysts and temperature may also trigger isomerization and cracking reactions that result in the production of uneven olefin molecules, as well as cyclic olefins or

even aromatics. However, such reactions are often pursued intentionally as they improve the jet fuel quality to meet standard and emission controls. In such sense, isobutanol, given its branched molecule character, presents additional benefits with respect to lighter (ethanol) or non-branched (1-butanol) alcohols derived from fermentative processes. Branching can indeed improve properties related to freezing point and cold flow properties.

The last relevant catalytic step in ATJ route is the hydrogenation unit, used to saturate the olefin double bond after oligomerization. This intends to reach nearly complete olefin hydrogenation to ensure a low jet fuel reactivity into undesired reactions. Hydrogen is fed in excess amounts and the reaction is catalyzed by Ni-based catalysts.[24] The unreacted $H_2$ is separated in relatively simple gas-liquid separation units, allowing its recycle and compression. The source of $H_2$ may be diverse, but ATJ biorefineries may benefit from lignin residuals left from saccharification and fermentation, which after gasification produce significant amounts of $H_2$. Such strategy, however, is not that common on existing ethanol facilities (from sugars) retrofitted for ATJ, as the remaining solids are used to produce distiller's grain.

**Commercial scale ATJ examples**

An overview of the commercial ATJ processes can be found in Table 5. Any alcohol production process involves several steps from biomass pretreatment into the final product. As in the case for GEVO, the process allows the co-production of ethanol and isobutanol, even when only the larger alcohol is only used for SAF production. Several product purification stages yield the final alcohol products, and in addition, side products also have market feasibility, as shown in GEVO website.[25]

*Table 5: Alcohol-to-SAF production routes developed at commercial scale.*

| Type of process | Companies | Alcohol intermediate |
|---|---|---|
| Sugar fermentation | LanzaTech/PNNL, Vertimass | Ethanol |
| Gas fermentation | LanzaTech/PNNL | Ethanol |
| Sugar to butanol fermentation | GEVO | Isobutanol |
| Syngas to ethanol | PNNL | Ethanol |

The separation of alcohol products from the stream obtained from fermentation yields both economic inputs but also operational costs, which especially differ if ethanol or isobutanol are produced. The primary water/alcohol separation is performed via distillation, and the product purity is limited by the water/alcohol azeotrope. As for ethanol, only 95.6 wt.% can be achieved through distillation, requiring additional separation steps (driven by adsorption process over materials such as molecular sieves) to reach product purities above 99%. As for C4 alcohols, both n-butanol and isobutanol form a heterogeneous two-phase liquid azeotrope. The use of high purity alcohol streams demands decanters coupled to stripping columns. However, SAF production facilities may even stand water contents in the 1-5% range, avoiding the use of energy-intensive and costly distillation stages, especially taking into account that the dehydration catalysts used in SAF production processes are tolerant to significant amounts of water.

This process contains three catalytic units (see ref. [25]), designed specifically for each condition and catalytic material: an alcohol dehydration step to form the corresponding olefin, the oligomerization of the light olefin into the adequate range of SAF olefins, and their saturation of the double bond via a hydrogenation step. The last step is the separation of the synthetic paraffin product. Olefin oligomerization units are common in the chemical plants to produce molecules applied as liquid fuels (gasoline, diesel). This has generated knowledge and thus further tuning of catalytic conditions would allow the production of hydrocarbons in the SAF range. Such products predominantly contain a

mixture of synthetic paraffins in the kerosene range, which is later separated to adapt into required jet blend. The remaining cuts are targeted as naphtha and/or diesel range products.

Among the alcohol-derived SAFs available in the market, those from GEVO (from isobutanol) and LanzaTech (from ethanol) have achieved certified standards to blend up to 30% and 50% of their SAF with the fossil-derived kerosene, indicative of the market potential of such hydrocarbon mixtures.[26]

**Economic viability of the ATJ process**

One of the factors that limits the economic viability in ATJ units is the low biomass conversion yield into alcohol and the high energy consumption for purification stages of alcohol products. Reported works focus on optimizing specific units related to dehydration, oligomerization, and hydrogenation stages. In most cases, such improvements consist of process intensification, heat integration or the design of new catalysts in order to reach improve process aspects related to the high costs and alcohol productivity.[27] The composition of a biojet-fuel, mostly composed of hydrocarbons with boiling points in the range of C8 and C16 paraffins, is similar to those in conventional fossil jet fuel. The main distinction is that biojet-fuels do not contain aromatic compounds and have lower levels of branched hydrocarbons than fossil jet fuel.

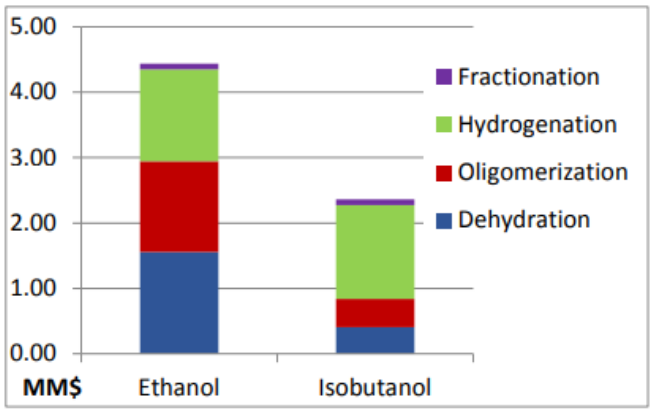


*Figure 1: Breakdown of process costs for SAF production from ethanol or isobutanol at a scale of 200 ton feed / day.*[18]

Light alcohols ($C_1$-$C_3$) can be produced from biomass through diverse catalytic routes, among which the most common ones are Fischer Tropsch, gasification, thermocatalysis or fermentation. Such alcohol diversity opens the spectrum of the types of feedstock to process through ATJ pathways, among which agricultural residues, sawdust, forest residues, carbohydrate-rich sources, straw, switchgrass or corn grains. Ethanol can be produced through fermentative process through relatively small-size sugars (as for starch crops) or complex mixtures (as derived from lignocellulosic biomass, microalgae), whereas isobutanol can be produced via fermentation using microbial strains and or carbonylation (chemical synthesis). The basic principle relies on alcohol dehydration over catalysts to form olefins. Oligomerization steps grow light olefins into larger oligomers, whereas hydrocarbon fuels require the deoxygenation and hydrogenation of these olefins during hydrotreatment steps.[28]

The fuels produced via ATJ routes yield minor amounts of particulate matter and sulfur oxides, but especially they outstand because their renewable character reduced at least 80% the $CO_2$ life cycle emissions. This leads to ATJ fuels with higher minimum selling price (MFSP), given the lower conversion yields and costs associated with feedstock extraction or fermentation steps. For instance, ATJ-SPK presents higher MFSP values than Jet A-1 and GFT-SPK fuels, even if having better performance in C-use and thermal efficiency. Techno-economic combined with environmental analyses on FT and ATJ routes from solid-wastes[29] indicated that biojet fuels present higher costs than standard jet fuel. On

the other hand, such FT or ATJ routes reduce 40-60% GHG emissions. Such reduction leads to a 93% rise in net present value.[30]

### 2·2·2 Alcohols from syngas

Most of knowledge in alcohol production from syngas is achieved for methanol formation via catalytic pathways, especially using natural gas or some other C-rich feedstock (coal, biomass). Such non-biological route to produce ethanol can be carried out via ethylene hydration (at 300 °C and 60–70 atm) using steam. The analogous ethanol productivity from syngas is, however, less explored. For such purpose two main routes are considered, which distinguish predominantly given their direct or indirect character, which uses methanol and dimethylether as intermediates (Figure 2).

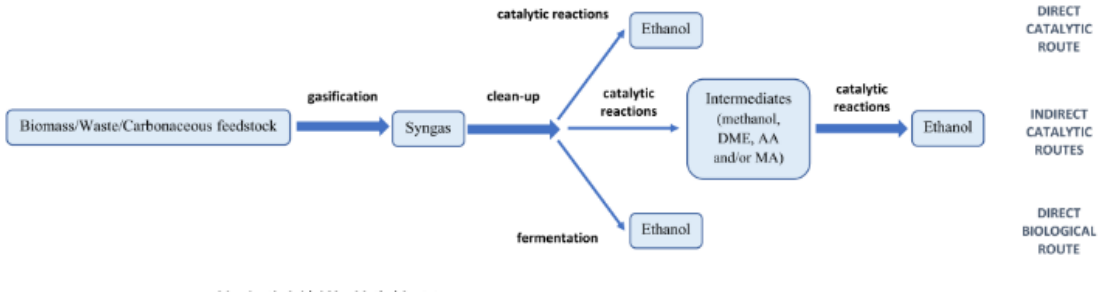


*Figure 2: Direct syngas-to-ethanol pathway.*

The direct pathway is energetically demanding and, given the numerous side-reactions, it produces ethanol with selectivity at high CO/CO2 hydrogenation conversion, especially in the form of methane, larger hydrocarbons or oxygenates. This scenario significantly increases the downstream separation costs.[33] Ethanol selectivities of 40% were reported but at <10% conversion, which complicates its industrial implementation. Rh-based catalysts show higher C2 oxygenate selectivity, but their larger costs (as compared to Co-based materials) makes them not viable at large scale. Indeed, the direct conversion of syngas to higher alcohols shows higher TRL than ethanol, which is still being developed under lab-scale TRL.[33] The development of C3-C4 alcohols suffers from higher selling prices. Thus research targets focus on tuning adequate catalysts towards higher activity, stability and selectivity. As alternative, indirect syngas-to-ethanol routes have been considered as viable and mature technologies.

**The methanol route for syngas-to-ethanol production**

One of the indirect pathways has been recently commercialized to convert waste into syngas,. Which is first used to produce methanol and then ethanol. This has been achieved by Enerkem in Canada using municipal solid waste. The economics of a plant processing 100,000 t of dry municipal solid waste per year and 38,000 $m^3$ ethanol production are positive, thanks to reduced operational costs and fiscal benefits.[34]

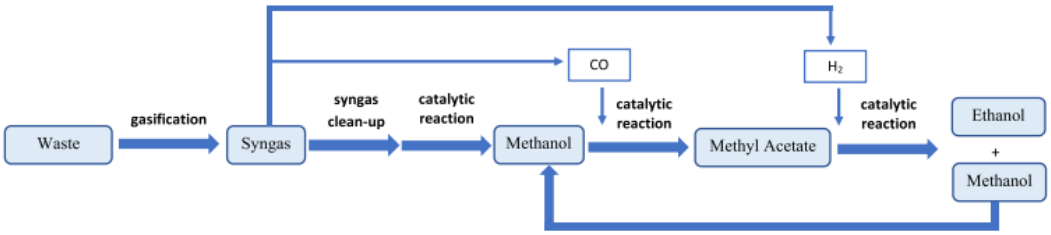


*Figure 3: Indirect syngas-to-ethanol pathway.*

The presence of $CO_2$ (below 10%) in the $Co/H_2$ mixture is beneficial for optimal catalyst activity during methanol production. $H_2/CO$ ratio of 2 is optimal for complete methanol conversion, which can also alternatively adjusted for an $(H_2+CO_2)/(CO+CO_2)$ ratio of 2. Cu-, ZnO-, $Al_2O_3$- or MgO-based catalysts outstand to catalyze such reactions. Even when ethanol selectivity is less than expected, methanol is also an interesting molecule in the chemicals industry or to produce dimethylether. Ethanol is produced from methanol by mixing with CO in fixed-bed reactor containing a Rh-based catalyst and methyl iodide as co-catalyst. The produced methylacetate is mixed with $H_2$, obtaining ethanol and methanol (as side-product). Such carbonylation reactions are mature under commercial scale, making the process economically viable.[35]

# 3 Direct syngas-to-Jet

A key challenge in FTS technology remains the single-pass conversion of syngas into a specific range of $C_n$ hydrocarbons with tunable selectivity considering ASF distribution rule. Conventional FTS products currently undergo further refining e.g., hydrotreatment (HT) to improve selectivity for the desired liquid fuels. Compared to this multi-step, energy-intensive process, directly producing specific liquid fuel ranges from syngas offers significant potential for improved energy efficiency and economic viability or at least modifying the conventional approach to have less steps. Deviation from the ASF distribution is crucial for having an applicable one step process. Bifunctional catalysts made from an FTS active catalyst (based on Fe, Co, Ni or Ru) combined with another phase which is active for hydrotreatment (HT: hydrocracking, hydro-isomerization) are reported for this objective.

In recent years, academic work has been published on developing bifunctional catalysts that combine FTS with HT for liquid fuel production. It was believed that typically hydrotreatment with precious metal/zeolite would not work under typical FTS conditions, due to lower pressure, lower temperature, low $H_2$ partial pressure and active site poisoning CO in the gas. However, if the HT catalyst is to be modified to work in combination with an FTS catalyst in the same reactor, then the advantages include, no wax formation, high per pass conversion, a simple product slate, no additional downstream conversion units and no high-pressure pure hydrogen required.

To accomplish this goal, conventional FTS catalysts can be integrated with a zeolite phase which are active for hydrotreatment. Other oxides and carbon-supported catalysts are also investigated but to a lesser extent than zeolites for having dual functionality. As mentioned, the acidic sites of zeolite (Bronsted acid sites) are active in (hydro)cracking and iso(oligo)merization as explained by Sartipi et al. [36] Cracking of wax and heavy hydrocarbons, and oligomerization of light hydrocarbon both are beneficial to deviate from ASF distribution and possibly increase the selectivity towards jet fuel range hydrocarbons. Interestingly, the FTS syngas and products are relatively clean and free from sulfur/nitrogen containing compounds therefore the hydrocracking can be performed under relatively mild conditions (conditions similar to that of LTFT reaction). This without poisoning zeolitic domains or the active phase of the FTS active phase.[36] The waxy products of FTS catalysts are also highly active for hydrocracking. A study by Sartipi et al.[37] proves that only zeolites with strong acid sites (and not weak-moderate ones), perform hydrocracking at the LTFT condition, which results in deviation from the ASF distribution.

These acidic zeolites can be combined with FTS catalysts in different ways as listed below; Each of these approaches results in different functionality.

| | |
|---|---|
| Dual bed | Two separated beds are utilized inside one reactor |
| Physical mixing | FTS and HT active phases are mixed and used in one bed |
| Core-shell | One of the FTS or HT active phase is coated with the other |
| Supported catalyst | FTS active metal is dispersed on the HT catalyst (or vice versa) |

## 3.1 The dual bed configuration

The advantage of the dual-bed configuration is that both catalysts are separated from each other and therefore possible migration of active metal species to other functional sides is limited. For instance, it is reported that alkali metals such as K can migrate from alkali promoted Fe based FTS catalyst to to the zeolite when they are in direct contact (physical mixing). Alkali metals reduce the acidity of zeolites by exchanging with the protons from Bronsted acid sites. The alkali migration leads to a decrease in activity and a shift in selectivity towards producing less valuable, lighter paraffinic products like methane. Compared to the dual-bed configuration, these drawbacks make physical mixing less

desirable.[36] Similar configurations with more complicated designs are also mentioned in literature known as layer by layer and multi-bed configuration.[38]

## 3.2 Physical mixing of catalysts

On the contrary to dual bed configuration, physical mixing can promote the synergy of having dual functionality in proximity. Moreover, sintering of FTS catalysts is limited in physical mixing configuration. For instance, it has been reported that physical mixing resulted in higher CO conversion than dual bed and selectivity of $C_5$-$C_{11}$ are improved in both Fe-based and Co-based FTS catalyst mixed with zeolites. Branching is also more common in physical mixing while the presence of heavier hydrocarbons like $C_{20+}$ are more common in dual-bed configuration. On the other hand, methane and $C_1$ products are more abundant in the physical mixing configuration. While the exact mechanism is not yet fully understood, acid cracking, hydrocarbon hydrogenolysis, heat effects, etc. are hypothesized. Adding diluent and heat conducting materials to mixed catalyst systems can reduce/eliminate extra methane formation indicating that this methanation is probably caused by local high temperatures caused by the high overall exothermicity (note that in addition to FTS reaction, the hydrocarbon hydrogenolysis over metal sites is also exothermic and higher temperatures increase methanation over FTS). [36] The core-shell (coated catalysts) and supported catalyst systems are even more selective than physical mixing to obtain $C_5$-$C_{11}$.[36]

Another example of the successful use of physical mixing of two catalysts has been reported.[39,40] A fuel selectivity of 70% was achieved at 225-260°C applying mixed FTS+HT catalysts in different configurations (face-to-face, dual-layer and hybrid). The system was tailored for liquid fuel production, not to specific transportation fuels.

## 3.3 Core shell catalysts

In the core-shell configuration, high selectivities to isoparrafins products have been obtained, especially when zeolitic membrane (HT active layer) fully cover the FTS catalyst surface. However, diffusion limitations of CO can result in a lower CO conversion than conventional FTS catalysts. Moreover, high methane selectivities are often found for this type of catalyst. In the core-shell catalysts, spatially confinement effect and shape selectivity occurred in a consecutive reaction specially if shell layer is micro/meso-porous materials.[41] Moreover, entrapping the FTS catalyst in the core of the structure can reduce the chance of its sintering. Such miniaturized capsule catalysts are prepared to realize efficient synthesis of liquid fuel with specific hydrocarbon distribution directly from syngas.[42] From a preparation point of view, exposing the FTS catalyst core to hydrothermal and alkali-rich conditions needed for the synthesis of the zeolite shell, already affect the FTS catalyst core. Specifically, silica supports in FTS catalysts can be dissolved during the zeolite preparation process, so the core can be involved in zeolite formation. Using an additional barrier coating before zeolitic shell preparation is reported as a solution for this problem in literature.[43] Alternatively, a metal organic framework or other coordination polymers are used as a core and after coating with shell layer (e.g. silica or zeolite), post calcination decompose the metal (FTS active one) containing framework to obtain metallic core.[44,45] Advanced characterization of prepared structures is necessary to understand and confirm the core-shell structure formation. Unknown lifetime of these catalyst in reaction condition is another limitation of this catalyst which need further studies.[36]

The research group of Tsubaki at the university of Toyama, reported one of the earliest Core-shell structures with an FTS active core and zeolite shell.[41,46] They prepared $Co/Al_2O_3$@H-beta capsule catalysts to realize iso-paraffin (primarily gasoline) production directly from syngas ($CO+H_2$). H-Beta zeolites were applied as membrane coating, which not only added hydrocracking and isomerization functionality but its confinement effect and shape selectivity also helped to obtain hydrocarbon products with a narrow distribution between $C_4$-$C_{12}$ (peaked at $C_7$).[41] Similarly, they also used H-ZSM-5

as a membrane shell to obtain middle isoparrafin products between $C_2$-$C_{10}$ (peaked at $C_5$).[46] As expected, the ZSM-5 based shell resulted in smaller hydrocarbon products than that with a zeolite beta shell due to the smaller pores in ZSM-5. Nonetheless, both core-shell structures differ from the mixed catalysts with similar zeolite-FTS catalyst ratios. In the core-shell structure, shape selectivity is more pronounced and there is a sharp cut off in chain length with the isoparafins selectivity two-three times higher than that of the physically mixed system.

Core-shell structures using silica instead of a zeolite shell are also reported. For instance, Yang et al. [47] prepared Co nanoparticles encapsulated with a silica shell with different thicknesses, and they showed that a thinner layer of silica is beneficial for high FTS activity since it can inhibit oxidation of Co nanoparticles. Moreover, the absence of wax was also found beneficial due to less mass transfer limitations.

Extraordinary and relatively expensive methods to prepare core-shell catalysts are also reported.[44] The MOF-derived hollow void catalyst Co@C@Void@$CeO_2$ modified with ruthenium (Ru) was applied as an effective catalyst for FTS reaction.[44] The cobalt-carbon core is a degraded ZIF-67 MOF formed by calcination of prepared structure. The optimal catalyst performance prepared by this system reached a $C_{5+}$ hydrocarbons selectivity of 92% at a CO conversion of 90.3% ($C_{11\text{-}20}$: 54% and $C_8$-$C_{16}$: >65%).

Similarly, Qin et al.[45] reported on the synthesis of hollow Co@$SiO_2$ using ZIF-67 as template which was calcined to form hollow structure. This catalyst reached a high $C_{5+}$ hydrocarbons selectivity of 93.3% with methane selectivity below 3.4% in FTS with implemented experimental details in their study. ZIF-67 crystals in addition to acting as preliminary core, also helped to have high metal loading and great metal dispersion in obtained carbon-cobalt core.

## 3.4 Bifunctional catalysts

Using zeolites (or other HT active materials) as support for FTS active metals and their dispersion on them is another possibility. In this case, a few limitations should be considered. Co clusters formed inside the zeolite micropores are not FTS active due to strong metal-support interaction which decreases the reducibility of metals and due to small size of clusters which are reported to be less active (not optimal) in FTS reaction. For these reasons mesoporous zeolites are utilized and since high level of meso-porosity is required to have enough activity usually combination of both desilication (by alkali solutions) and dealumination by acidic treatment implemented to form enough mesoporisity in the zeolitic support. The acidity level and strength can also be tuned towards a desired value by these processes. Organic bases such as tetrapropylammonium (TPAOH) are favored over NaOH for alkali treatment and desilication, especially for less stable zeolitic framework (e.g., zeolite with high Al content such as zeolite Y). Treatment with strong bases can also decrease the crystallinity of zeolite and therefore reduce the acid catalyzed reaction activity. As mentioned earlier, strong acidity is required for bifunctional zeolite-FTS catalyst combinations with required cracking activity and dealumination (specially removing extra framework aluminum) by acid treatment using $HNO_3$, resulting in strong acid sites, especially in case of mesoZSM-5 catalysts.[36] From FCC catalyst research, it is well known that the presence of rare earth elements such as La and Ce can increase the hydrothermal and chemical stability of the zeolitic framework.[48] Such stabilization procedure expected to be useful in bifunctional catalysts used for FTS and indeed some papers have reported the incorporation of the rare-earth elements in the zeolitic framework.[49] Proximity of acid site and FTS component affect the product selectivity zeolite-FTS component catalysts with more olefinic product at shorter distance. Methane selectivities are also remarkably high in this case. Similar to core shell-structures, the lifetime of this type of bifunctional catalyst is unclear based on available literature.

Co loaded mesoporous H-ZSM-5 have been reported to be about three times more active than conventional Co-$SiO_2$ catalyst at comparable stability. With a $C_5$-$C_{11}$ selectivity above 60% on this catalyst and the suppression of wax formation.[36] Sartipi et al.[50] used hexane cracking on the

bifunctional FTS catalysts to study both hydrocracking and hydroisomerization of the zeolitic domain. Additionally, using ammonia TPD, they observed strong acid sites in mesoZSM-5 while only moderate and weak acid sites were present in meso-Y and meso-MOR. They found also that strong acid sites are necessary for cracking(hydrocracking) while acid sites with moderate strength are only active for isomerization under LTFT conditions.[37] They reported that low acidity and small zeolite crystals are preferred for a long catalyst lifetime in the presence of desirable cracking activity. For gasoline production, the mesoZSM-5 was optimal while they did not observe any cracking or isomerization by zeolite Y (also tested by hexane cracking reaction). Similarly, Boymans et al.[51] have also tested cobalt containing zeolitic framework with mesoporisity as bifunctional catalyst in the LTFT reaction. They also did not observe good activity with Co/meso-Y while with the use of Co/mesoZSM-5 and Co/meso-Beta catalyst, jet fuel range product with total selectivities of respectively 30.4% and 41.0% were obtained. We speculate that the low hydrothermal stability of zeolite Y was also the reason for this observation especially because water is also co-produced in FTS. In another research paper by Sartipi et al., they applied 10% Co/H-ZSM-5 catalyst with the hierarchical mesopores ZSM-5 zeolite to produce gasoline range products.[52] They showed that introducing mesoporosity in the zeolite increased not only the selectivity of gasoline range hydrocarbons, but also the CO conversion compared to a standard $Co/SiO_2$ reference catalyst. No wax was produced with the zeolitic catalysts. With $Co/SiO_2$, a $C_5$-$C_{11}$ selectivity of 27% was obtained compared to 51% of $C_5$-$C_{11}$ selectivity for hierarchical Co/H-ZSM-5. Unfortunately, more $C_1$-$C_4$ was produced over zeolitic catalysts. Test experiments revealed that not only hydroisomerization, but also extra hydrocracking occurred on the catalyst. They showed that the $C_1$ formation does not directly correlate with support acidity, but with direct CO hydrogenation which could be dominated by microporosity and $H_2$ diffusion. The strong Co-zeolite interaction gives lower coordinated Co sites and therefore a higher methane yield was observed.[52] However, it has been shown that vicinity of FTS and acid function – i.e. hybrid catalysts – perform better than physically mixed or layered catalyst beds related mostly to the hydrotreatment where Pt – $H^+$ should be close to enhance fast H/DH to allow higher HC to be cracked.

Xing et al. investigated the impact of zeolite properties, including acidity, pore structure, and mass ratio on isoparaffin production during FTS.[53] They employed $Co/SiO_2$ catalysts combined with Beta, ZSM-5, and SAPO-11 zeolites. Their findings suggest that large-pore acidic zeolites promote the formation of multi-branched alkanes by enabling closer proximity of molecules, facilitating the isomerization process. Conversely, strong acid sites were found to excessively crack long-chain hydrocarbons into shorter ones.

A 7.5 wt% Co–0.2 wt% Ru-catalyst, on $Al_2O_3$- ZSM-5 support, was reported by Kibby et al. to have a stable performance and high selectivity to $C_5$–$C_{20}$ up to 1500 h on-stream at 493 K. In case of the supported catalyst, it should be noted that coke formation was amplified under HTFT conditions[54] and therefore LTFT is preferred when acid catalysts are involved to inhibit deactivation of the catalyst.

Bifunctional catalysts including H-ZSM-5 have been reported frequently for the production of gasoline range hydrocarbons such as by Sartipi et al.[36] and others.[37,55,56]

For instance, Kang et al. reported on mesoporous supported ZSM-5[55] for the production of $C_5$–$C_{11}$ isoparaffins. They found that introducing mesoporisity in ZSM-5 is crucial to obtain high selectivity of $C_5$-$C_{11}$ (>58%) which was achieved through applying different concentrations of NaOH [0.1-0.5M] resulting in different levels of mesoporisity.

Though reports on bifunctional zeolites, such as those from Sartipi et al. and others[37,52,54] are a good examples of deviating from the ASF distribution, they are mostly aimed for gasoline and sometimes diesel fuels, and not for jet fuels. Tsubaki's group at the University of Toyama is one of the leading groups in direct production of jet fuels using novel integrated FTS catalysts.[3,41,42,49,57] To obtain jet fuel range fraction using zeolite containing FTS catalyst, large pore zeolites (e.g., Y and Beta) with enough cracking activity was found to be required. The challenge with ZSM-5 is that larger hydrocarbons will be trapped in the narrow zeolite channels where they undergo excessive isomerization and cracking.[50]

Li et al. reported the direct production of jet fuel from syngas with integrated Co/Ymeso-La catalyst.[49] Series of Co/ Ymeso-Ce, Co/Ymeso-La and Co/Ymeso-K catalysts were obtained by separate ion exchange of $Ce^{4+}$, $La^{3+}$ and $K^{+}$ into the parent mesoporous Y-type zeolite in their report. Both Co/mesoY-Ce and Co/mesoY-La catalysts shows higher selectivity of liquid fuels ($C_5$–$C_{20}$) with a higher $C_{iso}/C_n$ ratio(ratio of isoparaffin to n-paraffin) than the Co/Ymeso-Na catalyst. In detail, Co/Ymeso-Ce was found to be more selective to gasoline hydrocarbons (74%), while Co/Ymeso-La was found to be useful for producing jet fuel (72%). The isoparaffin-rich products will promote the octane number for gasoline products and decrease the freezing point of jet fuel, increasing the quality of the obtained fuels. Co/Ymeso-K showed a diesel fuel selectivity of 58%, while the $C_{iso}/C_n$ ratio was below 0.4, which well agrees with the criterion of high-quality diesel fuel. [3,49] The direct production of up to 72% jet fuel is the theoretical maximum in a sequential 2-step approach with α=0.87.[49] For jet fuel, they applied 15% Co/mesoY-La catalyst at 250°C, 20 bar and a $H_2$/CO of 1 at 40% CO conversion. The authors reported that the over-cracking to $C_1$-$C_4$ is prevented by the catalyst mesoporosity in combination with a decrease in Bronsted acidity by ion exchange of Zeolite HY with Na/La/Ce cations. Interestingly, the $H^{+}$ form is not required for hydrocracking, and the ion-exchanged form blocks cracking to lower range hydrocarbons.

In the same report, Li et al. proposed a new model to predict the distribution of products on bifunctional catalytic which also accounts for the cracking of heavier hydrocarbons, and can ease future catalyst designs.[49] The chain growth probability (a) and cracking contribution degree (b), was determined by employing the α value and various product selectivity for the Co/mesoY catalysts, are proposed as two important parameters. Both of those should be carefully checked to increase the desired products.

Zhuo et al. performed a similar study only by replacing the zeolite Y with Beta (Y, Ce, or La-modified Co/H-β), however, they aimed for gasoline production.[58] Similarly, Peng et al. reported diesel fuel production over mesoporous zeolite-Y-supported cobalt nanoparticles.[59]

While most bifunctional (or tandem) catalysts for direct jet fuel production are based on FTS active phase and zeolites, other alternatives are also reported instead of zeolites to prepare them. Here some of those system will be mentioned:

Ruthenium nanoparticles supported on carbon nanotubes were reported for diesel production by Kang et al.[60] The Ru/CNT catalyst showed high selectivity for $C_{10}$–$C_{20}$ hydrocarbons (diesel fuel). They observed that the $C_{10}$–$C_{20}$ selectivity strongly depended on the mean size of the Ru nanoparticles. Nanoparticles with a mean size around 7 nm exhibited the highest $C_{10}$–$C_{20}$ selectivity (ca. 65 %) at a relatively high turnover frequency for CO conversion. They attributed this high diesel selectivity to the adsorbed hydrogen species and the acidic functional groups on CNT surfaces which may both play roles in moderate hydrocracking of heavy hydrocarbons ($C_{10}$–$C_{20}$). They also found that by tuning the size of Ru particle they can tune the selectivity.

A Co/$ZrO_2$-$SiO_2$ catalyst with a specific bimodal structure has been reported for jet fuel production by Tsubaki's. However this catalyst was investigated in special FTS conditions accompanied with 1-olefin addition.[3,57] Nonetheless, the catalyst was found more active than conventional monomodal catalyst according to their report. They attributed this higher activity to the catalyst's bimodality. The large pores offer pathways for fast diffusion to obtain a high $C_{5+}$ selectivity and low $CH_4$ selectivity, while the small pores of catalyst provide a high active surface area to enhance the catalytic activity.

Yuan et al. [61] used machine learning for syngas to $C_{5+}$ fuels elaboration and finding optimal conditions though their conclusion was opposite to some of the experimental reports. For instance, it has been reported that larger particles of Co trapped in core-shell structure are more beneficial for diesel and long chain hydrocarbon formation while the opposite was predicted in this paper.[3,62]

Cheng et al. reported on confined cobalt nanoparticles within silica by entrapping cobalt particles inside porous silica, referred to as watermelon seeds approach.[63] They managed to tune selectivity from diesel-range hydrocarbons (66.2%) to gasoline-range hydrocarbons (62.4%) using this catalyst by

adjusting the crystallite sizes of confined cobalt inside silica from 7.2 to 11.4 nm and therewith deviate from the ASF law.

## 3.5 Co-feeding of 1-olefins and syngas

Introduction of small amount of 1-olefins (e.g., 1-octene, 1-decene, 1-tetradecene) together with syngas to in FTS was reported to significantly alter the product distribution, shifting it towards a jet fuel-like composition.[57,64,65] This approach achieved:

- Jet fuel selectivity exceeding 65%, a substantial improvement over traditional FTS process.
- In case it aimed for gasoline, the product selectivity can reach 91%.

Iglesia et al. discovered that re-absorbing alpha-olefins, byproducts of Fischer-Tropsch synthesis, leads to the re-growth of alkyl chains on the surface and the formation of larger hydrocarbon molecules.[66,67] This idea was later used by others [57,64,65] to add 1-olefins and therefore to increase the chain length of FTS products. The presence of 1-olefins in the feedstock likely acts as a chain growth promoter, deviating from the ASF distribution and favoring heavier hydrocarbons. Furthermore, subsequent hydrogenolysis reactions can shorten long-chain molecules while secondary hydrogenation converts olefins to paraffins.[57]

A pilot scale BTL unit has been constructed using this approach by Tsubaki's group for the production of SAF. This unit exhibits outstanding performance, delivering a jet fuel production rate exceeding 700 $g \cdot kg_{cat}^{-1} \cdot h^{-1}$ with a biomass consumption of just 240 $kg \cdot d^{-1}$.[16]

Yang et al. [68] study the effect of co-feeding of ethylene over conventional Co-based FTS catalysts and they observed faster hydrogenation of ethylene than CO and observed increased branching in the presence of ethylene.

# 4 Syngas-to-olefins(-to-jet)

Our literature survey has indicated that modified FTS catalysts toward olefins can be used indirectly to produce jet fuels after an additional oligomerization and hydrogenation step. Alternatively, syngas to olefins via non-FTS routes are also reported. Therefore, literature relevant to these options will be discussed in this part followed by a brief summary of olefin oligomerization and hydrogenation to obtain jet fuels.

## 4.1 Fischer-Tropsch to olefins (FTO)

The majority of FTS catalyst reported for light olefin production (FTO) are based on Fe as they are more selective to olefins, oxygenate and aromatics. This also indicates that most of the catalysis is performed in HTFT condition. Here, we tried to review some of the benchmark catalysts reported for this reaction. A review paper by Galvis and de Jong lists and compares most of FTO catalysts till publication date up to 2013.[69] in their review they categorize most important catalyst with high $C_2$-$C_4$ olefin selectivity at different temperature and CO conversions (Figure 4).

Considering this review, Fe–Mn–K/Sil-2[70] and Fe–Mn/MgO[71] catalysts have a enhanced catalytic performance when the FTO reaction was performed with a $H_2$/CO ratio of 2 while the Fe–Na–S catalysts supported on CNF or α-$Al_2O_3$[72] shows a high activity even when using syngas with a $H_2$/CO ratio of 1.[69]

De Jong's group[72] also reported on sustainable and efficient catalysts for olefin production from syngas based on iron nanoparticles modified by sulfur and sodium and homogeneously dispersed on weakly interactive α-alumina or carbon nanofiber supports.[69,72–74] Their best catalyst reached 60% weight selectivity of $C_2$-$C_4$ olefins.

Alternatively, Amoo et al. [75] reported on a catalyst based on Fe nanoparticles fixed in nanosized carbon with a grown zeolite Y layer. These Fe nanoparticles embedded in zeolite Y microcrystals showed selectivities higher than 37% at a CO conversion of 91.2% for light olefin production.

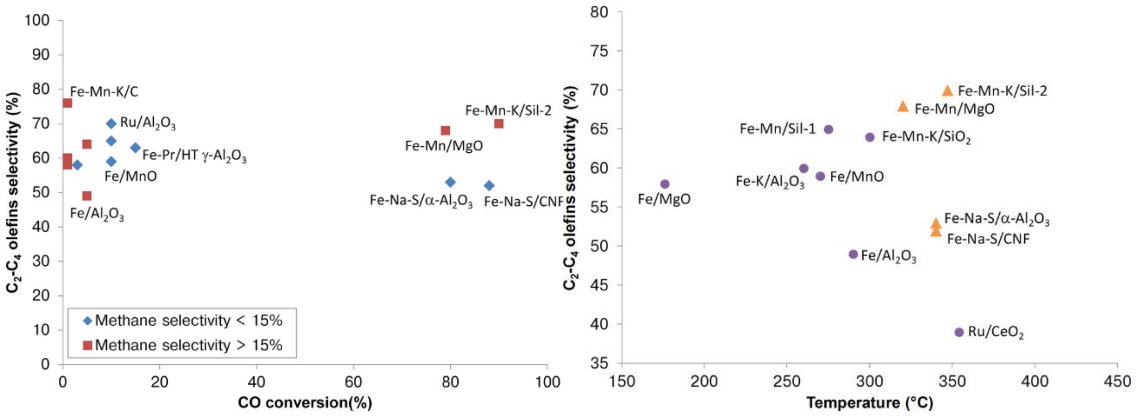


*Figure 4: selected catalysts for the FTO with a C2–C4 olefins selectivity above 50% (left). Selected catalysts with CH4 selectivity's below 15%-diamond, Selected catalysts with olefins selectivity above 35%-square. And low olefins selectivity's as a function of temperature (right): with low CO conversion (70%)-triangles.* [69]

Core-shell catalysts were shown to deviate from the ASF distribution and depending on the core, such multifunctional catalysts can be active to produce olefins, oxygenates, fuels or aromatics.[76] Similar to reported in the previous section, Tsubaki's group also reported core-shell structures highly active for FTO.[43] Fe/$SiO_2$-silicalite-1 zeolite capsule catalyst were reported by this group for light alkenes production. While they observed less CO conversion on core-shell structures (probably due to lower

CO diffusion). A $C_2$-$C_4$ olefin selectivity up to 45 % was obtained over a Fe/$SiO_2$-silicalite-1 zeolite capsule, which is almost twice of what they measured for conventional Fe/$SiO_2$ catalyst.

## 4.2 Syngas-to-olefins using non-FTS catalysts

In a perspective article in Science in 2016, K. P. de Jong[77] selected a publication on the conversion of syngas to olefins by Jiao et al. as a promising alternative to FTO and methanol to olefins (MTO).[77,78] In that report, $C_2$-$C_4$ olefins were obtained in an step from syngas over a $ZnCrO_x$/MSAPO catalyst. A selectivity of 74% $C_2$-$C_4$ olefins was obtained over a ZnCrOx--mSAPO catalyst (25 bar $H_2$/CO = 2.5, 400°C, 17% CO conversion). This was higher than the highest 61% reported for FTO at that time, as summarized in de Jong review paper.[69] Although the mechanism has not yet been elucidated, it must be different from the FTS mechanism as $CO_2$ is formed as the main by-product instead of $H_2O$ (probably through methanol as intermediate). This system involved a composite catalyst containing a spinel-structured oxide (ZnCrOx) and a mesoporous SAPO zeolite (MSAPO) with a hierarchical pore structure.[78] This achievement surpassed previously reported values in similar processes and exceeds the theoretical maximum for $C_2$-$C_4$ hydrocarbons in traditional FTS.

Key findings from this work include:

- **High C2=C4 selectivity:** The composite catalyst demonstrated significantly higher selectivity for C2=C4 olefins compared to both existing methods and theoretical predictions.
- **Low methane and heavier hydrocarbon formation:** Methane and heavier hydrocarbons ($C_{5+}$) were both below 5%, which is considerably lower than typical FTS processes.
- **Stable performance:** The catalyst displayed good reproducibility and maintained stable performance over a 110-hour test.

More recently, in 2022, a Na-Ru/$SiO_2$ catalyst was reported by Yu et al. [79] for very high olefin production (>80%) from syngas at low $CO_2$ production. This was enabled by sodium-promoted metallic ruthenium (Ru) nanoparticles with neglegible WGS reactivity, $CH_4$ and $CO_2$ production (<4%). Na-Ru/$SiO_2$ catalysts with 5% of theoretic weight of Ru loading and 0.5 molar ratio of Na/Ru was tested at 533 K, 1.0 MPa and $H_2$/CO ratio of 2. On the other hand, this catalyst is also producing larger olefin while the ox-zeo catalyst and Zn containing ones are more selective to $C_2$-$C_4$ olefins. Having different olefin distribution may affect the efficiency of catalyst in consequent oligomerization unit for jet fuel production.

Combining methanol synthesis and methanol to olefin (carbon-carbon coupling) catalysts is also reported for olefin production. The Zr–Zn binary oxide shows high selectivity to methanol and dimethyl ether even at 673 K, and after modification with SAPO-34 zeolite offers around 70 % selectivity for $C_2$–$C_4$ olefins at 10 % of CO conversion. The proximity of the components enhance the lower olefin selectivity.[80] It has been also reported that the conventional route to olefin through DME is more selective than some of these benchmark catalysts and for commercialization comparison with this option is crucial.[69]

Core shell structures are also useful for non-FTS syngas to olefin reactions. One-step synthesis of light olefins from syngas using Zn-Cr-O@SAPO34 capsule catalysts was also reported by Tsubaki's group.[81] In a recent report, this group reported core-shell structures with a $ZrO_2$@FeCu-K composition which exhibited an superior catalytic performance at a 97 % CO conversion and 49 % α-olefins selectivity by increased CO adsorption due to the $ZrO_2$ shell.[82] It should be noted that the reaction mechanism on these catalyst is different than for traditional FTS catalysts. The Zn-Cr catalyst produces methanol which can be dehydrated and converted to olefins when SAPO layer. Cheng et al.[80] also reported the preparation of similar catalysts containing mixed oxides of Zn-Zr and SAPO-34 however not in the form of core-shell (they prepared a composite catalyst). The Zr–Zn binary oxide alone have higher selectivity for methanol and dimethyl ether at moderate temperature (e.g., 673 K), and then the dehydration-

oligomerization on SAPO-34 (with decreased acidity) resulted in around 70 % selectivity for $C_2$–$C_4$ olefins at 10 % CO conversion.

Carbon-supported catalysts were also reported by a few research groups for olefin production. The advantage of carbon-based support is high dispersion and metal loading capability. Iron on nitrogen rich mesoporous carbon (NMC) has been reported by Tsubaki's group for light olefins production which showed high productivity above 3.2 g $HCh^{-1}$ $g_{Cat}^{-1}$ (highest reported iron-based catalyst, CO conversion>86%, $C_2$-$C_4$ olefins selectivity=31.7% ).[3,83] In another research[84], they also prepared Fe-Mn-rGO catalysts and investigated the ratio of Mn promoter to Fe to obtain high productivity. They found out that a Mn/Fe ratio of 16/100 gives a good olefin yield of 19% with an olefin/paraffin (O/P) ratio of 0.77.

Zhu et al. reported carbon-mediated strategy (using glucose as the carbon precursor) to construct supported Co-MnOx nano-interfacial catalyst that enables highly selective synthesis of long-chain linear α-olefins ($C_{5+}$=) via the Fischer-Tropsch (FT) reaction.[85]

In another report, a Pd/$SiO_2$@S1@H-ZSM-5 dual-shell capsule catalyst was synthesized using a dual-layer crystal growth method with an auxiliary hydrothermal reaction. The catalyst exhibits excellent selectivity to liquefied petroleum gas in $CO_2$ hydrogenation reactions, which is attributed to well-matched tandem reactions between methanol synthesis on the Pd/$SiO_2$ core catalyst and methanol dehydration to hydrocarbons on the H-ZSM-5 zeolite shell.[86] We are mentioning this catalyst in this section since olefin as intermediate is formed during methanol dehydration.

## 4.3 Olefin oligomerization and hydrogenation

Several types of solid acids have been identified as potential oligomerization catalysts, including phosphoric acid-silica, ion-exchanged resins, amorphous aluminosilicates, zeolites, acidic clays, and sulfated metal oxides.[87]

The mechanism of oligomerization differs depending on the type of active site. Bronsted acid sites in zeolites favor a "carbenium route," while metal sites can facilitate "metallacycle" or "Cossee-Arlman" mechanisms. While various metals have been used for olefin oligomerization, nickel is particularly common, including in homogeneous catalysts employed in the Shell High Olefins Process (SHOP). [87] $Ni^{2+}$ is reported to be active for oligomerization, with exchanged $Ni^{2+}$ appearing more active than Ni in NiO clusters or grafted $Ni^{2+}$.[88]

Although many metal catalysts, based on either metallacycle or Cossee-Arlman mechanisms, have been explored, those containing both metal and acid sites have seen extensive use, especially for ethylene oligomerization, which is challenging with solely acidic sites. [87]

Most studies have employed feeds with relatively high olefin content, as in the COD and MOGD processes. However, de Klerk and colleagues recently demonstrated using MFI zeolite to oligomerize a dilute (around 7%) $C_2$-$C_4$ containing Fischer-Tropsch (FT) tail gas fed into fuels, even in the presence of CO poisons. Interestingly, no CO interaction with olefins nor impact on olefin conversion was observed.[89]

Highly acidic sulfated and tungsten containing metal oxides have been implemented together with nickel to create bifunctional oligomerization catalysts. For instance, supported $NiSO_4$ on γ-$Al_2O_3$ containing $Fe_3O_4$ used as a Ni-sulfated alumina catalyst for FCC cracked olefin ($C_5$/$C_6$ olefins) oligomerization. Diesel yield depended on nickel amount, with 7 wt% achieving an optimal 45% yield. [87]

Nickel on tungstated alumina increase isobutene dimerization, exhibiting up to 80% selectivity towards octenes with sol-gel synthesized catalysts. The reaction temperature of 150 °C yielded the highest dimer selectivity, while the catalyst preparation method significantly impacted its stability.

Impregnated catalysts displayed a decrease in dimer selectivity with increasing temperature (50-150 °C), similar to observations with previously studied sulfated titania supported catalysts. [87]

Harvey et al. used a series of processes to create distillate fuels. Ethylene was first converted to hexene using a metallacycle derived trimerization catalyst. Then, a Dicaprazirconium Dichloride Activated with Methylaluminoxane catalyst converts 1-hexene to branched molecules with $C_{12}$-$C_{18}$. Previously, they demonstrated converting 1-butene to a 2-ethylhexene via a similar process, followed by acid treatment to transform the $C_8$ molecules into jet fuels.[90–92]

Babu et al. [93]: Researchers achieved ethylene-to-jet fuel conversion through a combined approach. Nickel supported on Al-containing SBA-15 transformed ethylene into liquids rich in $C_8$ molecules at 200 °C/10 bar and a WHSV of 0.38 $h^{-1}$. These liquids were then oligomerized using Amberlyst-35, leading to an overall jet fuel yield of around 42%.

Drab et al. [94] used $C_2H_4$ obtained from $CO_2$ hydrogenation to oligomerize it to jet fuel range materials with the yield of 56% using pelletized amorphous silica–alumina (ASA)-supported Ni catalysts (max conv.=64%, max sel. to jet=86%).

Dimethylether (DME) to Jet Fuels:[95] Researchers proposed a hypothetical process for DME conversion to jet fuels. Specific branched olefins, derived from acid-catalyzed DME processing, were oligomerized using Amberlyst-35 to distillate range oligomers with a specific yield at a specific temperature, accompanied by some isomerization and cracking.

Highly reduced supported nickel, Raney Nickel and precious metal (Pd, Ir) based catalysts are efficient to hydrogenate the remaining olefin in the feed to ensure all products are parafinic.[96–98] Since hydrogenation is relatively easier than syngas to olefin and olefin oligomerization reaction, in this section, we only mentioned some of the traditional catalyst for hydrogenation. Interestingly, hydrogenation can be performed at room temperature over Ni/C (nickel-graphitic shell-based core–shell-structured catalyst) catalyst which indicate the ease of the reaction.[99]

# 5 Syngas-to-alcohols(-to-jet)

As discussed in Chapter 2, there is currently no industrial-scale process for producing aviation fuels from syngas via alcohols. Commercial processes are divided into two categories: the production of methanol from syngas, and the production of aviation fuels from alcohols derived from fermentation, such as ethanol or isobutanol.

Therefore, it is necessary to unify a route for the production of aviation biofuels from syngas via alcohols. In this regard, this chapter will aim to gather the latest developments by dividing the process into ethanol production from syngas, followed by the dehydration of this alcohol to ethylene, and finally oligomerizing ethylene to produce jet range olefins.

## 5.1 Syngas to ethanol

The primary limitation of this stage for its industrial viability lies in its low conversion and selectivity. Consequently, multiple investigations have been undertaken with the aim of optimizing the catalytic system to improve both activity and selectivity towards ethanol. Recently, an exhaustive review has been published, focusing on the latest advances in the (catalytic) reaction mechanism for ethanol synthesis from syngas.[100]

The direct synthesis of alcohols from syngas entails two key processes: carbon chain growth and alcohol formation. Therefore, catalysts featuring active sites capable of dissociative adsorption of CO to promote chain growth, and active sites capable of non-dissociative CO adsorption for alcohol formation, are required.[101] Furthermore, it is important to achieve precise ethanol growth and prevent the production of other alcohols in order to achieve a high selectivity towards the desired product, which remains a significant challenge to date.[31,100]

The reaction is complex because it involves many intermediate elementary steps. Therefore, there is extensive research dedicated to studying ethanol production through indirect pathways via methanol or dimethyl ether (DME) production. However, these approaches involve multi-step processes that are energy-intensive due to the separation and purification requirements at each stage. Although this pathway will not be discussed in this chapter, a brief overview is provided, focusing on the tandem catalyst proposed by Kang et al. [31] due to its promising outcomes.

Integrating methanol synthesis, methanol carbonylation, and acetic acid hydrogenation into a single reactor was achieved through catalyst optimization for each step. The proposed tandem catalyst demonstrated a promising ethanol selectivity without requiring energy-consuming intermediate steps. The triple tandem system was composed of ZnO-$ZrO_2$ modified with K, which improved methanol selectivity, optimized H-MOR zeolite for increasing acetic acid selectivity, and Sn modified Pt/SiC for the hydrogenation (see ref. [31]). After optimizing the ratio of the three catalysts 9.7% CO conversion was achieved at an ethanol selectivity of 64%. Moreover, the catalyst exhibited high stability and no deactivation was observed in 100 h.[31]

To achieve economic feasibility, it is necessary to avoid high-energy-demand intermediate processes. In this sense, research on catalytic systems capable of synthesizing ethanol via the direct route is essential.

*Noble metal-based catalysts*

Rhodium (Rh) is known for its exceptional capability to dissociate CO and its high hydrogenation capacity. Employing unmodified Rh catalyst results in high yields of $CH_4$. However, as previously mentioned, non-dissociative CO adsorption is also necessary ethanol production. Consequently, Rh catalysts are modified with promoters and supports.

One of the most studied promoter for Rh-based catalysts is Fe.[102–105] *Haider et al.* investigated the improvement on the catalytic activity and selectivity of $Rh/SiO_2$ and $Rh/TiO_2$ in the presence of the Fe

promoter. After optimizing the Fe content, the maximum selectivity of 37% was achieved with 2%Rh-5%Fe/$TiO_2$, whereas the same catalyst without the promoter exhibited a selectivity of 11%. In both cases, the reached conversion did not exceed 7%. The enhanced selectivity of the catalyst was attributed to the close interaction between the metal and the promoter. However, elevated loadings of Fe suppressed the hydrogenation capacity of the catalyst by covering the active Rh surface.[106]

Similarly, Mn has been studied as promoter in Rh-based catalysts. The Mn-O-Rh interfacial structure played a crucial role in enhancing the selectivity of the catalyst, reaching 27.3% selectivity at 42.4% CO conversion. In the absence of a promoter, the conversion rate decreased significantly to 2.5%, with $CH_4$ being the predominant product, exhibiting a selectivity of 93.8%.[107]

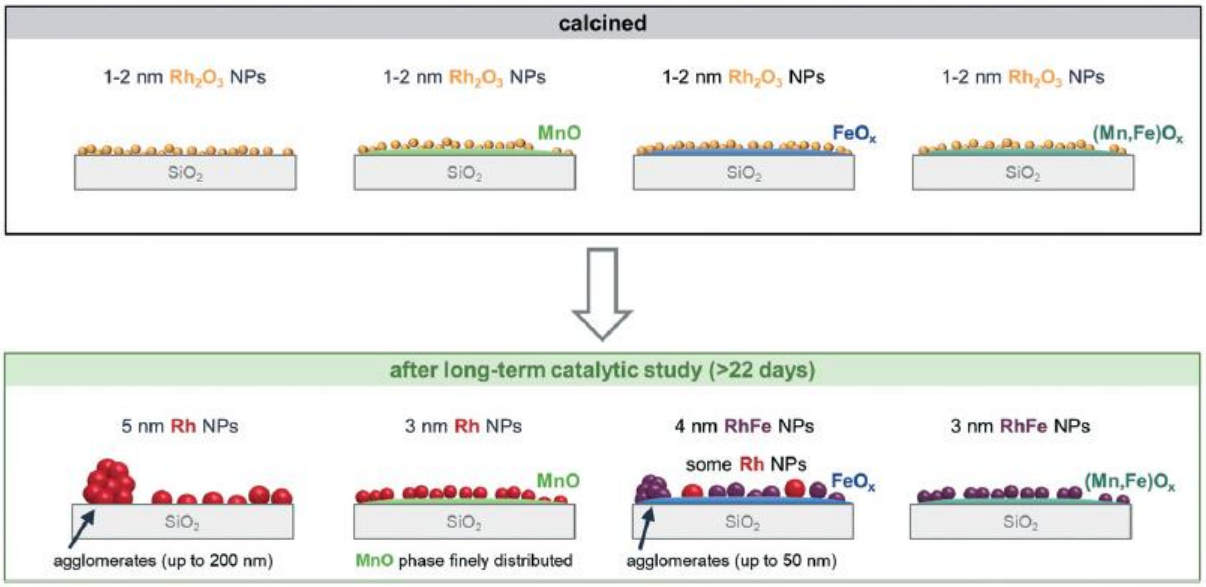


*Figure 5: Structural models after calcination and after long-term catalytic study.*[108]

Recently, the positive effect of both promoters has been studied.[109–111] MnO has been found to stabilize Rh nanoparticles, effectively preventing the agglomeration. The addition of Fe resulted in the formation of an Rh-Fe alloy, modifying the electronic properties of Rh/$SiO_2$ catalyst. Consequently, the RhMnFe/$SiO_2$ catalyst exhibited high selectivity to ethanol, attributable to the favourable influence of each promoter. Furthermore, it was evidenced that the utilization of both promoters concurrently enhanced the stability of the catalyst, as observed in Figure 5.[108]

Cu is also acquiring interest in the synthesis of ethanol from syngas. This metal has been extensively studied for methanol synthesis. Therefore, the coupling of chain growth active sites is necessary for the application of Cu-based catalyst in ethanol production. Cs and K were studied as promoters for alcohol production. A small amount of Cs was more favourable than K for the synthesis of ethanol and higher alcohols. At optimized reaction conditions, 41.6% CO conversion was achieved, reaching a maximum selectivity of 24.9% to the desired products.[112]

### *Non noble metal-based catalysts*

The catalysts based on non-noble metals are more appealing in terms of their industrial feasibility owing to their lower cost in comparison to noble metals.

Mo-based catalyst are promising non-noble metal catalyst for direct conversion of syngas to ethanol and have been extensible studied. Accordingly, the most active and selective catalyst will be outlined. $MoS_2$ based catalysts exhibit promising results. *Ferrari et al*. promoted the activity of bare $MoS_2$ by incorporating $K_2CO_3$ through physical mixing, enhancing the catalytic activity. The optimized catalyst

achieved a CO conversion of 20% with a selectivity of 20% towards ethanol.[113] Similarly, $MoS_2$ modified with K and Ni exhibited above 41% conversion and 42% selectivity to ethanol. The interaction effect of Ni and Mo resulted in the formation of the active phase $NiMo_3S_x$.[114] With the aim of avoiding sulphur-containing catalyst, other Mo-based catalyst have been investigated. Generally, the catalytic activity of the Mo-based catalyst proceeds the following order: $MoS_2 > Mo_2C > MoO_x > MoP$. However, they can be promoted with alkali and transition metals to enhance the activity of the catalyst.[115]

Traditionally, Co based catalyst have been employed for Fischer-Tropsch synthesis, as outlined in Chapter 2. Consequently, these calalysts exhibit active performance in CO dissociation and chain growth. Promoting these catalyst with active sites enhancing non-dissociative CO adsorption leads to active catalyst for the production of ethanol from syngas. The perovskite-structured catalyst synthetized employing La, Sr, Co and Ga exhibited high dispersion of Co and a strong interaction between Co and Ga. This strong interaction generated more Co-Ga active sites for alcohol synthesis, resulting in ethanol selectivity higher than 30%.[116] Recently, the effect of Ni on Co-$Co_2C$ catalyst was studied. It was concluded that CO was dissociatively adsorbed on metallic Co/Ni and non-dissociatively adsorbed on $Co^{\delta+}$-$Co_2C$ active sites. The active site proportion was modified by regulating Ni/Co ratio. When the ratio was effectively stablished, a maximum conversion of 12.8% was reached, reaching 19.4% ethanol selectivity.[117]

Lastly, the interaction between Cu and Co has been also reported, synergizing the role of Cu in methanol production with the role of Co in chain growth. Recently, Cu-Co interaction was studied on $Al_2O_3$ supported catalyst. The increase in the Cu ratio led to a higher selectivity toward alcohol, suggesting that the non-dissociative adsorption of CO on Cu sites was associated with alcohol formation. Additionally, it was found that dissociative CO adsorption occurred on Co. It was conclude that an optimal Co/Cu ratio with close Co-Cu proximity is neccesary for efficient synthesis of higher alcohols from syngas. In order to improve ethanol selectivity, a Co-Cu-Mn catalyst was synthetized. A total alcohol selectivity of 46.2% was achieved, with ethanol compromising 45.4% of the total alcohol products. These results represent an improvement in ethanol selectivity compared to Cu-Co based catalysts. The Mn species promote the activation of Cu and Co sites in the ternary CuCoMn system, enhancing the productivity of the catalyst.[118]

## 5.2 Ethanol dehydration to ethylene

Industrially, as discussed in Chapter 2, ethanol dehydration is performed using solid acid catalysts, with alumina and HZSM-5 zeolite being the predominant catalysts. Traditionally, $Al_2O_3$ has been employed for ethanol dehydration, and remains in industrial use. It exhibits moderate acidity and relatively good stability. However, elevated temperatures (300-500 °C) are needed to achieve optimal ethylene yield. More recently, HZSM-5 has gained attention for industrial application due to its high activity in ethanol dehydration. At lower temperatures (150-250 °C), the main product is diethyl ether. Consequently, higher temperatures (250-400 °C) are required for ethylene production. Moreover, strongly acidic zeolites exhibit inadequate time-on-stream stability.

Numerous research studies have been published demonstrating high conversions and selectivity to ethylene based on different acid catalysts such as $Al_2O_3$, $TiO_2$, or zeolites.[119] Current research efforts are focused on catalysts that exhibit stability and perform effectively under mild operating conditions.

### *Enhancing the catalyst stability*

*Hao et al*. reported a promising $Al_2O_3$-carbon catalyst modified with ammonia. The catalyst modified with ammonia exhibited a high conversion of 98.3% and an ethylene selectivity of 97%, compared with the sample without ammonia modification (63.2% and 46.7%, respectively) at 450 °C. The addition of ammonia generated Brønsted acid active sites, which remarkably enhancing the ethanol dehydration process. Moreover, adjusting the alumina content to 13.9% enhanced the number of weak acid active sites. This resulted in the development of a catalyst that was both active and stable for 144 h at reaction temperature.[120] Other metal oxides such as silica have also been studied. $Mn/SiO_2$ was synthetized, exhibiting a high selectivity to acetaldehyde. Upon modification of $SiO_2$ with $ZrO_2$, the increased acidity led to enhanced selectivity and stability. To further improve ethylene production, Fe, Ni and Zn were incorporated, with Ni exhibiting superior performance. The combination of Mn and Ni led to the development of a notably stable material over time on stream, with no observed decline in activity. It was concluded that the number of acid sites is correlated with the activity of the catalyst. Additionally, the ratio of weak to medium acid sites emerged as a critical factor for attaining high selectivity, with medium sites being a requirement.[121]

H-ZSM-5 modification has also been recently studied to improve the stability of the catalyst. Various Si/Al ratios were explored, along with Ce and Cu doping, to assess their impact on catalytic activity and stability. Varying the Al/Si ratio revealed that lower ratios increased activity due to increased acid site concentration. Additionally, Ce doping of HZSM-5 promoted higher desorption of reaction intermediates, increased the total acidity, and mitigated the generation of carbonaceous compounds. Consequently, higher stability over longer reaction times was achieved, up to 140 h, with almost complete conversion and 67% ethylene selectivity.[122]

In recent years, modified SBA-15 mesoporous silica has gained attention. *Cheng et al*. modified SBA-15 with palm oil clinker waste (POC) aiming to achieve a stable catalyst and develop a viable catalyst from agroindustrial waste. The modification with POC resulted in enriched weak-moderate acidity and lower strong acidity. The optimized catalyst was stable after 105 h on stream, reaching 73.33% conversion and 84.7% ethylene selectivity.[123] Similarly, the impregnation of tungsten into SBA-15 modified the acidity of the catalyst, enhancing both the catalytic activity and selectivity to ethylene. The optimized catalyst exhibited an increased Lewis to Brønsted acid ratio, which significantly influenced the catalytic dehydration of ethanol to ethylene. This resulted in the highest selectivity of ethylene (98.7%), with almost complete conversion of ethanol achieved at 400 °C.[124]

### *Optimizing catalyst performance under mild conditions*

Modifying H-ZSM-5 with a two step dealumination method resulted in enhanced catalytic performance during ethanol to ethylene dehydration process at low temperatures. This could be attributed to the tuned acidic sites, involving the reduction of strong acid sites exhibited by H-ZSM-5. The most

favourable ethylene yield and selectivity (98.5 and 100%) was obtained at 220 °C.[125] Similarly, H-ZSM-5 was modified using an alkaline solution (NaOH) to alter the physicochemical properties of the zeolite. It was observed that the Si and Al content, density of weak acid sites and the OH-treatment conditions, influenced the ethylene selectivity. This can be observed in Figure 6. Moreover, the cooperative effect of Brønsted and Lewis acid sites was confirmed, underscoring their significant role in the formation of ethylene from ethanol. When pure ethanol was fed, a maximum ethylene selectivity of 85% was achieved, with 60% ethanol conversion, at 225 °C.[21]

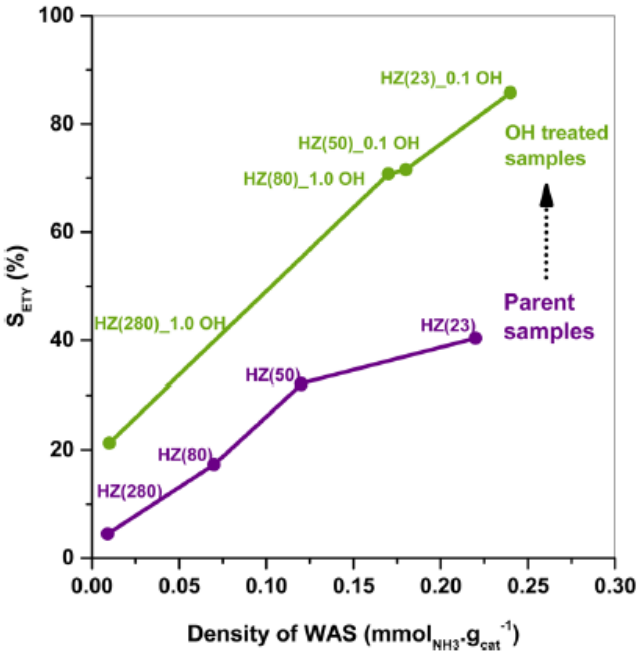


*Figure 6: Correlation between ethylene selectivity (at similar ethanol conversion) and the density of weak acid sites for parent (purple) and OH-treated (green) HZSM-5.[21]*

Rho type zeolite was synthetized, which showed lower pore size comparing to HZSM-5. In the mild conditions of ethanol dehydration, Rho exhibited superior overall catalytic efficiently compared to both commercial HZSM-5 and $Al_2O_3$ materials. The strength and concentration of solid-acid sites emerged as the dominant factor in the ethanol-to-ethylene dehydration process at low temperature. Consistently, the steady-state selectivity towards ethylene consistently exceeded 99% in the temperature range of 250-400 °C for the dehydration reactions.[126]

In recent years, an innovative perfluorosulfonic superacid (PFSA) resin has arisen as a favorable option for the mild condition dehydration of ethanol to ethylene. Concretely, Aquivion® PFSA was tested to explore the potential of this material. Moreover, the thermal properties and alcohol penetration into the resins were examined. The material exhibited excellent thermal stability up to 300 °C. Higher temperatures involved the beginning of the desulphonation process. Furthermore, the catalytic performance differed when varying from pellet to grains. Ethanol was observed to partially permeate the pellet structure, accessing the acid sites present in the material. Decreasing particle size enhanced the contact between ethanol and active sites, resulting in improved catalytic performance. The catalyst exhibited optimal behaviour at 200 °C, achieving nearly complete ethanol conversion and 90% ethylene selectivity.[127] One drawback of these materials is the low surface area they exhibit. To enhance the performance of Aquivion® PFSA resin, $TiO_2$ and $SiO_2$ were encapsulated within the resin. Concretely, $TiO_2$ exhibited the highest efficiency for ethanol conversion and ethylene selectivity at very low temperatures. When using pure Aquivion, minimal productivity was observed (0.05 $g_{ethylene}·min^{1}·g_{catalyst}$) due to mass transfer limitations. Upon optimizing the Aquivion/$TiO_2$ ratio, ethylene productivity increased up to 0.36 $g_{ethylene}·min^{-1}·g_{catalyst}$. The improved porosity and stability of the active sites enhanced the activity of the composites compared to the pure Adquivion® PFSA.

Lastly, certain authors are interested in investigating both stability and operation under mild conditions. Mesoporous aluminosilicates were synthetized to study stability at low temperature dehydration of ethanol to ethylene. The resulting aluminosilicates exhibited acidity between HZSM-5 and commercial silica, concerning acid sites strength and Brønsted to Lewis ratio. This yielded a stable material over time on stream, did not generate oligomers of ethylene , did not exhibited coke formation, with unchanged texture. In summary, they demonstrated outstanding resistance to coking. Despite exhibiting lower acidity compared to H-ZSM-5 due to their milder acidity, the conversion over H-ZSM5 notably decreased with time on stream due to coking. The mesoporous aluminosilicate demonstrated a gradual decline in ethylene selectivity, likely caused by the formation of diethylether. This phenomenon may be attributed to the *in situ* modification of the strongest Lewis acid sites, possibly due to presence of water.[128]

## 5.3 Ethylene oligomerization

Acid catalysed ethylene conversion is favoured at temperatures exceeding 300 °C. However, $C_{3+}$ olefins can oligomerize at lower temperatures (100-250 °C). Consequently, butenes emerged as the primary product of $C_2H_4$ oligomerization, exhibiting a significantly faster reaction rate than which react much more rapidly than $C_2H_4$. For optimal results, olefin oligomerization should occur at lower temperatures, promoting the formation of longer-chain olefins, while mitigating side reactions such as aromatization, transfer hydrogenation, and cracking.[129] However, transition metal based catalysts enable the oligomerization of ethylene at temperatures below 200 °C.[130] Generally, achieving high yields of jet fuel range products relies significantly on the use of highly selective catalysts.

### *Two-stage acid catalyzed oligomerization*

With the goal of enhancing the production of oligomers within the jet fuel range, *Babu et al.* proposed an integrated two-stage process. In the first stage, Ni-AlSBA-15 catalyst exhibited remarkable catalytic activity, achieving a conversion rate of over 99% ethylene, while yielding hydrocarbons with a non-Schulz-Flory type distribution ($C_8 > C_6 > C_4 > C_{10}$) and exhibiting high stability at 200 °C and 10 bar. Subsequently, the liquid mixture obtained in the first step underwent co-oligomerization using Amberlyst-35 ion-exchange resin. Operating conditions of 100 °C and 30 bar of $N_2$ yielded a liquid product ($C_{10} > C_8 > C_6 > C_4$) compromising over 98% $C_{5+}$, with $C_{10+}$ olefins accounting for approximately 42%.[93]

### *One-pot cascade ethylene oligomerization*

Another strategy that has been implemented to optimize selectivity towards jet-range products involves employing two catalysts in series within the same reactor. Compared to the catalytic results from reactions with the single catalysts under identical conditions, the one-pot cascade Ni/Siral-30 and HZSM-5 exhibited close to 100% conversion and resulted in a completely reversed Schulz-Flory type product distribution ($C_{10+} > C_8 > C_6 > C_4$), and yielded the highest amount of liquid product for the entire reaction time at 250 °C. First, each catalyst was tested independently at different reaction temperature. H-ZSM-5 was not reactive at temperature below 250 °C. Above 300 °C, the selectivity of $C_{10+}$ products was higher than Ni/Siral-30, but the ratio of non-cyclic linear hydrocarbons to aromatics was 10/90, contributing to a significant production of aromatics. On the contrary, Ni/Siral-30 exhibited a high conversion at low temperatures, but the selectivity of $C_{10+}$ was low. Thus, the combination of both catalysts could lead to jet-fuel range hydrocarbons production, while avoiding the formation of excessive aromatic products. At 250 °C, high ethylene conversion, selectivity to $C_{10+}$, and liquid yield was achieved, compared to 200 and 300 °C. Moreover, the H-ZSM-5 was treated with NaOH (HZSM-5-5B) to study the modification of the catalyst properties. Thereby, it was affirmed that the ratios of $C_{10-19}$ and $C_{20+}$, as well as non-cyclic linear hydrocarbons to aromatics, could be altered through the NaOH treatment of H-ZSM-5.[131]

In line with this strategy, *Mohamed et al.* proposed a dual-bed system. Initially, ethylene dimerization was performed using a Ni catalyst supported on H-Y zeolite, followed by oligomerization over a H-ZSM-5 zeolite. As depicted in Figure 7, the Ni/Y catalyst produces $C_4$ olefins, while H-ZMS-5 zeolite is essential for producing jet-fuel range products. Selectivity and deactivation of the catalyst were studied as a function of catalyst acidity, temperature and bed configuration. It was concluded that zeolites with higher acidity (lower Si/Al) enhanced the catalytic activity. Regarding catalyst deactivation, the dual-bed method demonstrated efficiency in preserving the oligomerization catalyst (H-ZSM-5) from deactivation due to coke deposition compared to the initial Ni/Y dimerization catalyst, which deactivates at a faster rate. Nevertheless, the catalysts are unable to maintain the activity over extended periods. With the optimized conditions, the dual-bed setup achieved a jet fuel range product selectivity exceeding 50% for over 20 hours. However, the ethylene conversion decreased significantly during the course of the reacton.[132]

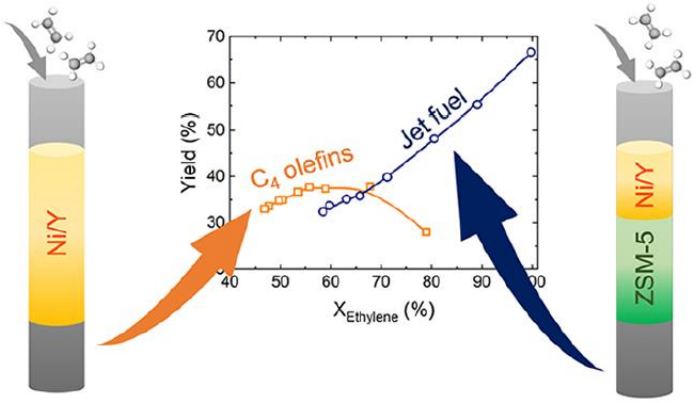


*Figure 7: Dual-bed strategy for enhancing jet-fuel range olefins.*[132]

## *One-pot direct oligomerization*

Several nickel-based catalysts supported on microporous aluminosilicates have been studied for ethylene oligomerization. Moon et al. conducted ethylene oligomerization using NiH- and H- forms of ZSM-5 and beta zeolite catalysts. The Si/Al and Ni content were maintained constant to study the differences in the textural properties. Crystal size and mesoporoity of the catalysts were varied through sophisticated constructive and destructive techniques. The combination of nanocrystallinity and intercrystalline mesoporosity obtained in the catalyst resulted not only in high initial activity and stability but also high selectivity towards jet fuel range products. The oligomerization of ethylene under 35 bar and 200 °C over the optimized catalyst exhibited remarkable $C_{10+}$ product selectivity higher than 80%.[133] With the aim of simplifying the catalyst synthesis, Ni was impregnated on a commercial SIRAL-30 support with a high Brønsted acid site density. The support exhibited a high Si/Al ratio, resulting in high surface acidity, which enhanced the activity of the catalyst. Moreover, optimal conversion and selectivity to $C_{10+}$ were achieved with a 4% Ni loading. Finally, pretreatment under $N_2$ atmosphere at 550 °C proved advantageous for enhancing both the dispersion of $Ni^{2+}$ species and Brønsted acid site density. Despite achieving relatively low selectivity (approximately 20%), the stability of this catalyst makes it a noteworthy system. Moreover, while some deactivation was observed in the used catalyst due to the adsorption of heavy oligomers, the initial catalytic activity was effectively restored by treating the catalyst at 550 °C in an air atmosphere.[134]

Being aware of the importance of Ni impregnation step, different catalyst were synthetized by both one-pot synthesis employing Ni-ligands and post-synthesis approach. The former method promoted the formation of NiO nanoclusters within the zeolitic pores. Conversely, the post-synthesis impregnation resulted in a higher content of $Ni^{2+}$ in ion exchange position, with the stabilization of these species being favoured for zeolites with higher Al content. It was demonstrated that the post-synthesis approach exhibited higher activity. However, higher selectivity to jet fuel range products was obtained when the catalyst was synthetized by one-pot employing Ni-ligands. Additionally, it was concluded that the size of the crystallites is pivotal, as nano-sized zeolites demonstrated greated activity and stability against deactivation. Therefore, the methodical synthesis of Ni-containing zeolites, managing both the zeolite structure and crystal size, as well as the Ni speciation and acidic characteristics of the support, enables the enhancement of both initial activity and catalyst life. The achieved maximum yield rose to 45% at 200 °C and 35 bar.[135]

Furthermore, mesoporous silica modified with aluminium has been investigated as a support. Subsequently, Ni was impregnated to alter the physicochemical properties. Ni-AlSBA-15 appeared as a promising catalyst for the oligomerization to produce biojet fuel range hydrocarbons. The selectivity towards $C_{10+}$ products was enhanced at higher temperatures, higher pressures and lower weight hourly space velocity (WHSV). Moreover, the catalyst demonstrated prolonged stability throughout long-term catalytic test.[136] Similarly, mesoporous Ni-AlKIT-6 was synthetized through wetness impregnation

method to load Ni. The effect of the Si/Al ratio was investigated, concluding that higher Si/Al ratio enhanced the ethylene conversion. The acidity of the catalyst varied according to the amount of Al integrated in the silica framework, where increased aluminium content led to decreased acid strength. Moreover, elevated Al content altered the structure of KIT-6, decreasing the catalytic activity. On the other hand, high acid strength promoted aromatic hydrocarbons. Thus, the optimal Si/Al ratio was determined to be 5.[137]

# 6 Conclusions and recommendations

An overview of the most relevant references can be found in Table 6. This Table allows to compare the different processes based on the selected criteria. In the selectivity column, the maximum carbon selectivity for only the first syngas conversion step can be found followed by an esimated commercial feasibility of the catalyst production. In the final two columns, the complete syngas-to-Jet process is considered showing the total required processing units, including the first syngas conversion step with additional units needed for e.g. oligomerization and hydrogenation. And in the last column, an estimation of the quality of the $C_8$-$C_{16}$ hydrocarbons in terms of branched alkanes is included.

One of the developments in the catalytic conversion of syngas involves the direct conversion of syngas into jet fuel range hydrocarbons (**syngas-to-SAF**). This is mostly based on FTS, but then combined with integrated hydrotreatment thereby indirectly deviating from the limiting ASF hydrocarbon distribution. Integration of both steps has been ongoing work in the literature with some of the best performing including La stabilized Co / meso-Y catalysts achieving up to 72% selectivity to C8-C16 under LTFT conditions.[49] Secondly, confined Co / $SiO_2$ in which the size of the Co crystallites, which are trapped within the $SiO_2$ support, can direct the hydrocarbon selectivity with an estimated maximum of 65% C8-C16 selectivity.[63] Also, core-shell Co catalysts[44] and carbon nanotube supported Ru[60] showed promising results at a maximum $C_8$-$C_{16}$ selectivity of 65% for both. Clearly an advantage of this direct syngas-to-SAF is the need for only 1 conversion unit, however, the catalyst production involves multiple synthesis steps or the use of expensive metals. Moreover, the catalyst stabililty in these mostly bifunctional catalyst systems is largely unreported and therefore unknown.

Alternatively, light olefins can be produced from syngas which can then be followed by oligomerization and hydrogenation to obtain the jet fuel range hydrocarbons (**syngas-to-olefins**). Promising recent work has been reported by the application of Na-Ru / $SiO_2$ in which 80% of $C_2$-$C_{20}$ olefins were obtained with only 3% $CO_2$ under LTFT conditions.[79] Other examples include work using metal oxides physically mixed with zeolites such as ZnCrOx—mSAPO, which achieved a $C_2$-$C_4$ olefin selectivity of up to 74% (25 bar $H_2$/CO = 2.5, 400°C, 17% CO conversion), however, with 45% $CO_2$ formation.[78] And, also published in 2016, a somewhat similar system and reaction conditions using ZnZrOx – SAPO achieving up to 80% $C_2$-$C_4$ olefins but also at high (45%) $CO_2$ formation.[80] For the syngas-to-olefin production routes, although selectivities to desired hydrocarbons is high (especially when not considering $CO_2$ production), consecutive oligomerization and hydrogenation will result in an overall carbon selectivity lower than that of the direct syngas-to-SAF approach. Moreover, even though considered established, the oligomerization in presence of syngas might result in unforeseen challenges. For these reasons we consider this approach as not (yet) ready for further development into a TRL-5 process towards improved SAF production.

Another potential approach involves synthesizing alcohols from syngas, followed by dehydration of the resultant alcohol, oligomerization, and hydrogenation processes, yielding aviation-range fuel (**syngas-to-alcohol**). Ethanol production is restricted by the low activity and selectivity reported in the literature. Catalyst based on noble metals, such as rhodium modified with molybdenum (Mn-O-Rh), demonstrated significant CO conversion (42.2%) and achieved a maximum ethanol selectivity of 27.3%.[107] To avoid the use of noble metals, $MoS_2$ modified with K and Ni was synthetized, exhibiting conversions above 41% and ethanol selectivity of 42%.[114] The dehydration stage represents a mature technology, with the water separation step being crucial as it can influence the catalyst activity and stability during oligomerization. The production of methanol is however commercial, which alcohol could also be converted to olefins (MTO) and SAF. However, the same reasoning can be applied here that the multiple post processing steps to obtain jet fuel hydrocarbons lower the overall carbon selectivity. Moreover, the once-through conversion level of syngas to MeOH are restricted due to the thermodynamic equilibrium.

As a recommendation of the approach with the greatest potential to follow for further development to TRL-5, we consider the confined Co / $SiO_2$ catalytic process. Based on the high selectivity to $C_8$-$C_{16}$ hydrocarbons (deviating from ASF) and the relatively straightforward catalyst preparation. Besides confirmation of reported conversions and selectivities, further developments need to include long term stability tests and determination and improvement of the fuel quality regarding branched $C_8$-$C_{16}$ alkanes.

*Table 6: Commercial and selected state-of-the-art examples of jet fuel synthesis from syngas and their rating based on the selection criteria.*

| | First syngas conversion step | | *Overall Syngas-to-Jet Process* | |
|---|---|---|---|---|
| **Approach / process** | **Selectivity (max.)** | **Catalyst production (complexity / commercial feasibility)** | ***Total conversion units*** | ***Final Jet fuel grade (branched C8-C16)*** |
| **Commercial SAF** | | | | |
| SMDS process (conventional) | 45% C8-C16 from syngas | Good | *2* | *Good* |
| ATJ "commercial" fermentation based[138] | 40% to C8-C16 from alcohol (ethanol) | Good | *4* | *Good* |
| **Syngas-to-SAF (direct)** | | | | |
| Co / La-meso-Y (Li et al., 2018)[49] | 72% C8-C16 | Poor | *1* | *Good* |
| Confined Co / SiO2 (Cheng et al, 2018)[63] | 65% C8-C16 | Good | *1-2* | *Unknown* |
| Core-shell Co@C@Void@CeO2 (Safari et al., 2023)[44] | 65% C8-C16 | Poor | *1-2* | *Unknown* |
| Ru / CNT (Kang et al., 2009)[60] | 65% C8-C16 | Poor | *1-2* | *Medium* |
| **Syngas-to-olefins** | | | | |
| Na-Ru / SiO2 (Yu et al., 2022)[79] | 80% C2-C20 olefins, 3% CO2 | Medium | *2-3* | *Good* |
| ZnCrOx – mSAPO (Jiao et al., 2016)[78] | 80% C2-C4 olefins, 45% CO2 | Medium | *3* | *Good* |
| ZnZrOx – SAPO (Cheng et al., 2016)[80] | 74% C2-C4 olefins, 40% CO2 | Medium | *3* | *Good* |
| **Syngas-to-alcohol** | | | | |
| Cu/ZnO/Al2O3 for syngas-to-methanol | 99.9% | Very good | *4* | *Good* |
| RhMn@S-1 (Wang et al., 2020)[107] | 27.3% | Medium | *4* | *Good* |
| K-$NiMo_3S_x$ (Wang et al., 2018)[114] | 42% | Medium | 4 | *Good* |

# 7 References


1. D02 Committee. *ASTM D7566: Specification for Aviation Turbine Fuel Containing Synthesized Hydrocarbons*. http://www.astm.org/cgi-bin/resolver.cgi?D7566-23B (2023) doi:10.1520/D7566-23B.
2. Okolie, J. A. *et al.* Multi-criteria decision analysis for the evaluation and screening of sustainable aviation fuel production pathways. *iScience* **26**, 106944 (2023).
3. Hondo, E., Lu, P., Zhang, P., Li, J. & Tsubaki, N. Direct Production of Hydrocarbons by Fischer-Tropsch Synthesis Using Newly Designed Catalysts. *J. Jpn. Pet. Inst.* **63**, 239–247 (2020).
4. Gholami, Z., Tišler, Z. & Rubáš, V. Recent advances in Fischer-Tropsch synthesis using cobalt-based catalysts: a review on supports, promoters, and reactors. *Catal. Rev.* **63**, 512–595 (2021).
5. Cheng, K. *et al.* Chapter Three - Advances in Catalysis for Syngas Conversion to Hydrocarbons. in *Advances in Catalysis* (ed. Song, C.) vol. 60 125–208 (Academic Press, 2017).
6. Dry, M. E. The Fischer–Tropsch process: 1950–2000. *Catal. Today* (2002).
7. Torres, 2013, Thesis FTO de Jong group.pdf.
8. Sie, 1991, Conversion of natural gas to transportation fuels via the SMDS.pdf.
9. Bouchy, C., Hastoy, G., Guillon, E. & Martens, J. A. Fischer-Tropsch Waxes Upgrading *via* Hydrocracking and Selective Hydroisomerization. *Oil Gas Sci. Technol. - Rev. IFP* **64**, 91–112 (2009).
10. Pearl GTL - overview | Shell Global. https://www.shell.com/what-we-do/major-projects/pearl-gtl/pearl-gtl-an-overview.html.
11. Gholami, Z., Tišler, Z. & Rubáš, V. Recent advances in Fischer-Tropsch synthesis using cobalt-based catalysts: a review on supports, promoters, and reactors. *Catal. Rev.* **63**, 512–595 (2021).
12. Sguazzin, A. The World's Biggest Emitter of Greenhouse Gases. *Bloomberg* (2020).
13. Myrstad, R., Eri, S., Pfeifer, P., Rytter, E. & Holmen, A. Fischer–Tropsch synthesis in a microstructured reactor. *Catal. Today* **147**, S301–S304 (2009).
14. LeViness, S. *et al.* Improved Fischer-Tropsch Economics Enabled by Microchannel Technology. (2011).
15. Piermartini, P., Boeltken, T., Selinsek, M. & Pfeifer, P. Influence of channel geometry on Fischer-Tropsch synthesis in microstructured reactors. *Chem. Eng. J.* **313**, 328–335 (2017).
16. Li, J. *et al.* Selectively Converting Biomass to Jet Fuel in Large-scale Apparatus. *ChemCatChem* **9**, 2668–2674 (2017).
17. Klerk, A. D. Fischer–Tropsch fuels refinery design. *Energy Environ. Sci.* **4**, 1177 (2011).
18. Geleynse, S., Brandt, K., Garcia-Perez, M., Wolcott, M. & Zhang, X. The Alcohol-to-Jet Conversion Pathway for Drop-In Biofuels: Techno-Economic Evaluation. *ChemSusChem* **11**, 3728–3741 (2018).
19. Wang, W.-C. *et al. Review of Biojet Fuel Conversion Technologies*. www.nrel.gov/publications. (2016).
20. Banzaraktsaeva, S. P., Ovchinnikova, E. V., Danilova, I. G., Danilevich, V. V. & Chumachenko, V. A. Ethanol-to-ethylene dehydration on acid-modified ring-shaped alumina catalyst in a tubular reactor. *Chem. Eng. J.* **374**, 605–618 (2019).

21. Ouayloul, L., El Doukkali, M., Jiao, M., Dumeignil, F. & Agirrezabal-Telleria, I. New mechanistic insights into the role of water in the dehydration of ethanol into ethylene over ZSM-5 catalysts at low temperature. *Green Chem.* **25**, 3644–3659 (2023).

22. Forestière, A., Olivier-Bourbigou, H. & Saussine, L. Oligomérisation des mono-oléfines par des catalyseurs homogènes. *Oil Gas Sci. Technol.* **64**, 649–667 (2009).

23. US8373012.

24. Alonso, F., Riente, P. & Yus, M. Transfer hydrogenation of olefins catalysed by nickel nanoparticles. *Tetrahedron* **65**, 10637–10643 (2009).

25. *AN OVERVIEW OF GEVO'S BIOBASED ISOBUTANOL PRODUCTION PROCESS ISOBUTANOL PRODUCTION PROCESS 1*. www.gevo.comwww.gevo.com (2023).

26. Okolie, J. A. *et al.* Multi-criteria decision analysis for the evaluation and screening of sustainable aviation fuel production pathways. doi:10.1016/j.isci.

27. Romero-Izquierdo, A. G., Gómez-Castro, F. I., Gutiérrez-Antonio, C., Hernández, S. & Errico, M. Intensification of the alcohol-to-jet process to produce renewable aviation fuel. *Chem. Eng. Process. - Process Intensif.* **160**, (2021).

28. Petersen, A. M., Chireshe, F., Okoro, O., Gorgens, J. & Van Dyk, J. Evaluating refinery configurations for deriving sustainable aviation fuel from ethanol or syncrude. *Fuel Process. Technol.* **219**, 106879 (2021).

29. Liu, G., Hagelin-Weaver, H. & Welt, B. A Concise Review of Catalytic Synthesis of Methanol from Synthesis Gas. *Waste* **1**, 228–248 (2023).

30. Luning Prak, D. J. *et al.* Physical and chemical analysis of alcohol-to-jet (ATJ) fuel and development of surrogate fuel mixtures. *Energy Fuels* **29**, 3760–3769 (2015).

31. Kang, J. *et al.* Single-pass transformation of syngas into ethanol with high selectivity by triple tandem catalysis. *Nat. Commun.* **11**, (2020).

32. Spivey, J. J. & Egbebi, A. Heterogeneous catalytic synthesis of ethanol from biomass-derived syngas. *Chem. Soc. Rev.* **36**, 1514–1528 (2007).

33. Xue, X. *et al.* Research progress of catalysts for synthesis of low-carbon alcohols from synthesis gas. *RSC Adv.* **11**, 6163–6172 (2021).

34. Marie-Rose, S. C., Chornet, E., Lynch, D. & Lavoie, J.-M. From biomass-rich residues into fuels and green chemicals via gasification and catalytic synthesis. *Trans. Ecol. Environ.* **143**, 1743–3541 (2011).

35. US8003822.

36. Sartipi, S., Makkee, M., Kapteijn, F. & Gascon, J. Catalysis engineering of bifunctional solids for the one-step synthesis of liquid fuels from syngas: a review. *Catal. Sci. Technol.* **4**, 893–907 (2014).

37. Sartipi, S. *et al.* Towards Liquid Fuels from Biosyngas: Effect of Zeolite Structure in Hierarchical-Zeolite-Supported Cobalt Catalysts. *ChemSusChem* **6**, 1646–1650 (2013).

38. Zhao, S. *et al.* Recent advances on syngas conversion targeting light olefins. *Fuel* **321**, 124124 (2022).

39. Sun, C. Direct syngas-to-fuel: integration of Fischer-Tropsch synthesis and hydrocracking in micro-structured reactors.

40. Kirsch, H., Lochmahr, N., Staudt, C., Pfeifer, P. & Dittmeyer, R. Production of CO2-neutral liquid fuels by integrating Fischer-Tropsch synthesis and hydrocracking in a single micro-structured reactor: Performance evaluation of different configurations by factorial design experiments. *Chem. Eng. J.* **393**, 124553 (2020).

41. Bao, J., He, J., Zhang, Y., Yoneyama, Y. & Tsubaki, N. A Core/Shell Catalyst Produces a Spatially Confined Effect and Shape Selectivity in a Consecutive Reaction. *Angew. Chem. Int. Ed.* **47**, 353–356 (2008).

42. Yamane, N. *et al.* Building premium secondary reaction field with a miniaturized capsule catalyst to realize efficient synthesis of a liquid fuel directly from syngas. *Catal. Sci. Technol.* **7**, 1996–2000 (2017).

43. Wang, Y. & Tsubaki, N. Powerful and New Chemical Synthesis Reactions from CO2 and C1 Chemistry Innovated by Tailor-Made Core–Shell Catalysts. in *Core-Shell and Yolk-Shell Nanocatalysts* (eds. Yamashita, H. & Li, H.) 105–120 (Springer, Singapore, 2021). doi:10.1007/978-981-16-0463-8_7.

44. Safari, M., Haghtalab, A. & Roghabadi, F. A. Promoting jet fuel production by utilizing a Ru-doped Co-based catalyst of Ru-Co@ C (Zd)@ Void@ CeO 2 in Fischer Tropsch synthesis. *RSC Adv.* **13**, 35525–35536 (2023).

45. Qin, C. *et al.* A high active sites exposed hollow Co@SiO2 nanoreactor for high performance fischer–tropsch synthesis. *Fuel* **323**, 124377 (2022).

46. He, J., Xu, B., Yoneyama, Y., Nishiyama, N. & Tsubaki, N. Designing a New Kind of Capsule Catalyst and Its Application for Direct Synthesis of Middle Isoparaffins from Synthesis Gas. *Chem. Lett.* **34**, 148–149 (2005).

47. Yang, J., Fang, X., Xu, Y. & Liu, X. Investigation of the deactivation behavior of Co catalysts in Fischer–Tropsch synthesis using encapsulated Co nanoparticles with controlled SiO 2 shell layer thickness. *Catal. Sci. Technol.* **10**, 1182–1192 (2020).

48. Vogt, E. T. C. & Weckhuysen, B. M. Fluid catalytic cracking: recent developments on the grand old lady of zeolite catalysis. *Chem. Soc. Rev.* **44**, 7342–7370 (2015).

49. Li, J. *et al.* Integrated tuneable synthesis of liquid fuels via Fischer–Tropsch technology. *Nat. Catal.* **1**, 787–793 (2018).

50. Sartipi, S., Parashar, K., Makkee, M., Gascon, J. & Kapteijn, F. Breaking the Fischer–Tropsch synthesis selectivity: direct conversion of syngas to gasoline over hierarchical Co/H-ZSM-5 catalysts. *Catal Sci Technol* **3**, 572–575 (2013).

51. Boymans, E., Nijbacker, T., Slort, D., Grootjes, S. & Vreugdenhil, B. Jet Fuel Synthesis from Syngas Using Bifunctional Cobalt-Based Catalysts. *Catalysts* **12**, (2022).

52. Sartipi, S. *et al.* Hierarchical H-ZSM-5-supported cobalt for the direct synthesis of gasoline-range hydrocarbons from syngas: Advantages, limitations, and mechanistic insight. *J. Catal.* **305**, 179–190 (2013).

53. Xing, C. *et al.* Syngas to isoparaffins: Rationalizing selectivity over zeolites assisted by a predictive isomerization model. *Fuel* **285**, 119233 (2021).

54. Kibby, C. *et al.* Chevron's gas conversion catalysis-hybrid catalysts for wax-free Fischer–Tropsch synthesis. *Catal. Today* **215**, 131–141 (2013).

55. Kang, J. *et al.* Mesoporous Zeolite-Supported Ruthenium Nanoparticles as Highly Selective Fischer–Tropsch Catalysts for the Production of C5–C11 Isoparaffins. *Angew. Chem. Int. Ed.* **50**, 5200–5203 (2011).

56. Sartipi, S. *et al.* Insights into the Catalytic Performance of Mesoporous H-ZSM-5-Supported Cobalt in Fischer–Tropsch Synthesis. *ChemCatChem* **6**, 142–151 (2014).

57. Li, J., Yang, G., Yoneyama, Y., Vitidsant, T. & Tsubaki, N. Jet fuel synthesis via Fischer–Tropsch synthesis with varied 1-olefins as additives using Co/ZrO2–SiO2 bimodal catalyst. *Fuel* **171**, 159–166 (2016).

58. Zhuo, Y., Zhu, L., Liang, J. & Wang, S. Selective Fischer-Tropsch synthesis for gasoline production over Y, Ce, or La-modified Co/H-β. *Fuel* **262**, 116490 (2020).

59. Peng, X. *et al.* Impact of Hydrogenolysis on the Selectivity of the Fischer–Tropsch Synthesis: Diesel Fuel Production over Mesoporous Zeolite-Y-Supported Cobalt Nanoparticles. *Angew. Chem. Int. Ed.* **54**, 4553–4556 (2015).

60. Kang, J., Zhang, S., Zhang, Q. & Wang, Y. Ruthenium Nanoparticles Supported on Carbon Nanotubes as Efficient Catalysts for Selective Conversion of Synthesis Gas to Diesel Fuel. *Angew. Chem. Int. Ed.* **48**, 2565–2568 (2009).

61. Yuan, Z., Wang, Y., Zhu, L., Zhang, C. & Sun, Y. Advancing C5+ hydrocarbons fuels production: An interpretable machine learning framework for Co-catalyzed syngas conversion. *Fuel* **361**, 130658 (2024).

62. Jiang, N. *et al.* A novel silicalite-1 zeolite shell encapsulated iron-based catalyst for controlling synthesis of light alkenes from syngas. *Catal. Commun.* **12**, 951–954 (2011).

63. Cheng, Q. *et al.* Confined small-sized cobalt catalysts stimulate carbon-chain growth reversely by modifying ASF law of Fischer–Tropsch synthesis. *Nat. Commun.* **9**, 3250 (2018).

64. Liu, X., Li, X. & Fujimoto, K. Effective control of carbon number distribution during Fischer–Tropsch synthesis over supported cobalt catalyst. *Catal. Commun.* **8**, 1329–1335 (2007).

65. Liu, X., Hamasaki, A., Honma, T. & Tokunaga, M. Anti-ASF distribution in Fischer-Tropsch synthesis over unsupported cobalt catalysts in a batch slurry phase reactor. *Catal. Today* **175**, 494–503 (2011).

66. Iglesia, E. Design, synthesis, and use of cobalt-based Fischer-Tropsch synthesis catalysts. *Appl. Catal. Gen.* **161**, 59–78 (1997).

67. Iglesia, E., Reyes, S. C., Madon, R. J. & Soled, S. L. Selectivity Control and Catalyst Design in the Fischer-Tropsch Synthesis: Sites, Pellets, and Reactors. in *Advances in Catalysis* (eds. Eley, D. D., Pines, H. & Weisz, P. B.) vol. 39 221–302 (Academic Press, 1993).

68. Yang, J. *et al.* The effect of co-feeding ethene on Fischer-Tropsch synthesis to olefins over Co-based catalysts. *Appl. Catal. Gen.* **598**, 117564 (2020).

69. Torres Galvis, H. M. & de Jong, K. P. Catalysts for production of lower olefins from synthesis gas: a review. *ACS Catal.* **3**, 2130–2149 (2013).

70. Xu-Longya, Wang-Qingxia, Xu-Yide, & Huang-Jiasheng. Promotion effect of K2O and MnO additives on the selective production of light alkenes via syngas over Fe/silicalite-2 catalysts. *Catal. Lett.* **31**, 253–266 (1995).

71. Xu, X. & Goodman, D. W. The effect of particle size on nitric oxide decomposition and reaction with carbon monoxide on palladium catalysts. *Catal. Lett.* **24**, 31–35 (1994).

72. Torres Galvis, H. M. *et al.* Supported iron nanoparticles as catalysts for sustainable production of lower olefins. *science* **335**, 835–838 (2012).

73. Galvis, H. M. T. *et al.* Effect of precursor on the catalytic performance of supported iron catalysts for the Fischer–Tropsch synthesis of lower olefins. *Catal. Today* **215**, 95–102 (2013).

74. Galvis, H. M. T. *et al.* Effects of sodium and sulfur on catalytic performance of supported iron catalysts for the Fischer–Tropsch synthesis of lower olefins. *J. Catal.* **303**, 22–30 (2013).

75. Amoo, C. C. *et al.* Fabricating Fe Nanoparticles Embedded in Zeolite Y Microcrystals as Active Catalysts for Fischer–Tropsch Synthesis. *ACS Appl. Nano Mater.* **3**, 8096–8103 (2020).

76. Lin, T. *et al.* Advances in Selectivity Control for Fischer–Tropsch Synthesis to Fuels and Chemicals with High Carbon Efficiency. *ACS Catal.* **12**, 12092–12112 (2022).

77. de Jong, K. P. Surprised by selectivity. *Science* **351**, 1030–1031 (2016).

78. Jiao, F. *et al.* Selective conversion of syngas to light olefins. *Science* **351**, 1065–1068 (2016).

79. Yu, H. *et al.* Direct production of olefins from syngas with ultrahigh carbon efficiency. *Nat. Commun.* **13**, 5987 (2022).

80. Cheng, K. *et al.* Direct and Highly Selective Conversion of Synthesis Gas into Lower Olefins: Design of a Bifunctional Catalyst Combining Methanol Synthesis and Carbon–Carbon Coupling. *Angew. Chem. Int. Ed.* **55**, 4725–4728 (2016).

81. Tan, L. *et al.* Design of a core–shell catalyst: an effective strategy for suppressing side reactions in syngas for direct selective conversion to light olefins. *Chem. Sci.* **11**, 4097–4105 (2020).

82. Guo, X. *et al.* Enhanced α-olefins selectivity by promoted CO adsorption on ZrO2@FeCu catalyst. *Catal. Today* **375**, 290–297 (2021).

83. Liu, G. *et al.* Nitrogen-rich mesoporous carbon supported iron catalyst with superior activity for Fischer-Tropsch synthesis. *Carbon* **130**, 304–314 (2018).

84. Nasser, A.-H. *et al.* Mn–Fe nanoparticles on a reduced graphene oxide catalyst for enhanced olefin production from syngas in a slurry reactor. *RSC Adv.* **8**, 14854–14863 (2018).

85. Zhu, M.-L. *et al.* Long-chain α-olefins production over Co-MnOx catalyst with optimized interface. *Appl. Catal. B Environ. Energy* **346**, 123783 (2024).

86. Li, H. *et al.* A Well-Defined Core–Shell-Structured Capsule Catalyst for Direct Conversion of CO2 into Liquefied Petroleum Gas. *ChemSusChem* **13**, 2060–2065 (2020).

87. Nicholas, C. P. Applications of light olefin oligomerization to the production of fuels and chemicals. *Appl. Catal. Gen.* **543**, 82–97 (2017).

88. Henry, R. *et al.* Ethene oligomerization on nickel microporous and mesoporous-supported catalysts: Investigation of the active sites. *Catal. Today* **299**, 154–163 (2018).

89. Halmenschlager, C. M., Brar, M., Apan, I. T. & de Klerk, A. Oligomerization of Fischer–Tropsch Tail Gas over H-ZSM-5. *Ind. Eng. Chem. Res.* **55**, 13020–13031 (2016).

90. Harvey, B. G. & Meylemans, H. A. 1-Hexene: a renewable C6 platform for full-performance jet and diesel fuels. *Green Chem.* **16**, 770–776 (2014).

91. Wright, M. E., Harvey, B. G. & Quintana, R. L. Highly Efficient Zirconium-Catalyzed Batch Conversion of 1-Butene: A New Route to Jet Fuels. *Energy Fuels* **22**, 3299–3302 (2008).

92. Wright, M. E., Harvey, B. G. & Quintana, R. L. Diesel and jet fuels based on the oligomerization of butene. (2013).

93. Babu, B. H., Lee, M., Hwang, D. W., Kim, Y. & Chae, H.-J. An integrated process for production of jet-fuel range olefins from ethylene using Ni-AlSBA-15 and Amberlyst-35 catalysts. *Appl. Catal. Gen.* **530**, 48–55 (2017).

94. Drab, D. M. *et al.* Hydrocarbon Synthesis from Carbon Dioxide and Hydrogen: A Two-Step Process. *Energy Fuels* **27**, 6348–6354 (2013).

95. Behl, M., Schaidle, J. A., Christensen, E. & Hensley, J. E. Synthetic Middle-Distillate-Range Hydrocarbons via Catalytic Dimerization of Branched C6–C8 Olefins Derived from Renewable Dimethyl Ether. *Energy Fuels* **29**, 6078–6087 (2015).

96. Lok, C. M. *Structure and Performance of Selective Hydrogenation Catalysts*. (De Gruyter: Berlin, Boston, 2018).

97. Bai, J., Tamura, M., Nakayama, A., Nakagawa, Y. & Tomishige, K. Comprehensive study on Ni- or Ir-based alloy catalysts in the hydrogenation of olefins and mechanistic insight. *ACS Catal.* **11**, 3293–3309 (2021).

98. Sebakhy, K. O., Vitale, G. & Pereira-Almao, P. Production of highly dispersed Ni within nickel silicate materials with the MFI structure for the selective hydrogenation of olefins. *Ind. Eng. Chem. Res.* **58**, 8597–8611 (2019).

99. Gao, J. *et al.* Ambient Hydrogenation and Deuteration of Alkenes Using a Nanostructured Ni-Core–Shell Catalyst. *Angew. Chem.* **133**, 18739–18746 (2021).

100. Liu, G., Yang, G., Peng, X., Wu, J. & Tsubaki, N. Recent advances in the routes and catalysts for ethanol synthesis from syngas. *Chem. Soc. Rev.* **51**, 5606–5659 (2022).

101. Mäki-Arvela, P., Aho, A., Simakova, I. & Yu. Murzin, D. Sustainable Aviation Fuel from Syngas through Higher Alcohols. *ChemCatChem* **14**, e202201005 (2022).

102. Gogate, M. R. & Davis, R. J. X-ray absorption spectroscopy of an Fe-promoted Rh/TiO2 catalyst for synthesis of ethanol from synthesis gas. *ChemCatChem* **1**, 295–303 (2009).

103. Han, T. *et al.* Rh-Fe alloy derived from YRh0.5Fe0.5O3/ZrO2 for higher alcohols synthesis from syngas. *Catal. Today* **298**, 69–76 (2017).

104. Liu, W., Wang, S., Sun, T. & Wang, S. The Promoting Effect of Fe Doping on Rh/CeO2 for the Ethanol Synthesis. *Catal. Lett.* **145**, 1741–1749 (2015).

105. Liu, Y. *et al.* Synthesis Gas Conversion over Rh-Based Catalysts Promoted by Fe and Mn. *ACS Catal.* **7**, 4550–4563 (2017).

106. Haider, M. A., Gogate, M. R. & Davis, R. J. Fe-promotion of supported Rh catalysts for direct conversion of syngas to ethanol. *J. Catal.* **261**, 9–16 (2009).

107. Wang, C. *et al.* Direct Conversion of Syngas to Ethanol within Zeolite Crystals. *Chem* **6**, 646–657 (2020).

108. Preikschas, P. *et al.* Formation, dynamics, and long-term stability of Mn- And Fe-promoted Rh/SiO2catalysts in CO hydrogenation. *Catal. Sci. Technol.* **11**, 5802–5815 (2021).

109. Damma, D., Boningari, T. & Smirniotis, P. G. Multimetallic Rh-La/M/SiO2 (M = W, V, Ce, and Zr) catalysts for oxygenates synthesis from syngas. *Chem. Eng. Sci.* **243**, (2021).

110. Liu, J. *et al.* Correlating the degree of metal-promoter interaction to ethanol selectivity over MnRh/CNTs CO hydrogenation catalysts. *J. Catal.* **313**, 149–158 (2014).

111. Pan, X. *et al.* Enhanced ethanol production inside carbon-nanotube reactors containing catalytic particles. *Nat. Mater.* **6**, 507–511 (2007).

112. Sun, J., Wan, S., Wang, F., Lin, J. & Wang, Y. Selective Synthesis of Methanol and Higher Alcohols over Cs/Cu/ZnO/Al2O3 Catalysts. *Ind. Eng. Chem. Res.* **54**, 7841–7851 (2015).

113. Ferrari, D. *et al.* Effect of potassium addition method on MoS2 performance for the syngas to alcohol reaction. *Appl. Catal. Gen.* **462–463**, 302–309 (2013).

114. Wang, N. *et al.* Enhanced catalytic performance and promotional effect of molybdenum sulfide cluster-derived catalysts for higher alcohols synthesis from syngas. *Catal. Today* **316**, 177–184 (2018).

115. Luk, H. T., Mondelli, C., Ferré, D. C., Stewart, J. A. & Pérez-Ramírez, J. Status and prospects in higher alcohols synthesis from syngas. *Chem. Soc. Rev.* **46**, 1358–1426 (2017).

116. Guo, S. *et al.* Mixed Oxides Confined and Tailored Cobalt Nanocatalyst for Direct Ethanol Synthesis from Syngas: A Catalyst Designing by Using Perovskite-Type Oxide as the Precursor. *Ind. Eng. Chem. Res.* **57**, 2404–2415 (2018).

117. Wang, J. *et al.* In situ topochemical carbonization derivative Co-Ni alloy@Co-Co2C for direct ethanol synthesis from syngas. *Appl. Surf. Sci.* **557**, (2021).

118. Sun, K. *et al.* Design and synthesis of spherical-platelike ternary copper-cobalt-manganese catalysts for direct conversion of syngas to ethanol and higher alcohols. *J. Catal.* **378**, 1–16 (2019).

119. Xie, S., Li, Z., Luo, S. & Zhang, W. Bioethanol to jet fuel: Current status, challenges, and perspectives. *Renew. Sustain. Energy Rev.* **192**, (2024).

120. Hao, Y. *et al.* Hierarchical leaf-like alumina-carbon nanosheets with ammonia water modification for ethanol dehydration to ethylene. *Fuel* **333**, (2023).

121. Florea, M. *et al.* Tuning the acidity by addition of transition metal to Mn modified hollow silica spheres and their catalytic activity in ethanol dehydration to ethylene. *Appl. Catal. Gen.* **646**, (2022).

122. Quiroga, E. *et al.* Industrial crude bioethanol dehydration to ethylene: Doping ZSM-5 to enhance selectivity and stability. *J. Environ. Chem. Eng.* 111803–111803 (2023) doi:10.1016/j.jece.2023.111803.

123. Cheng, Y. W. *et al.* Ethylene production from ethanol dehydration over mesoporous SBA-15 catalyst derived from palm oil clinker waste. *J. Clean. Prod.* **249**, (2020).

124. Trongjitraksa, P., Klinthongchai, Y., Praserthdam, P. & Jongsomjit, B. Elucidation on supporting effect of WO3 over MCF-Si and SBA-15 catalysts toward thanol dehydration. *J. Taiwan Inst. Chem. Eng.* **152**, (2023).

125. Wu, C. Y. & Wu, H. S. Ethylene Formation from Ethanol Dehydration Using ZSM-5 Catalyst. *ACS Omega* **2**, 4287–4296 (2017).

126. Masih, D., Rohani, S., Kondo, J. N. & Tatsumi, T. Catalytic dehydration of ethanol-to-ethylene over Rho zeolite under mild reaction conditions. *Microporous Mesoporous Mater.* **282**, 91–99 (2019).

127. Andreoli, S. *et al.* Superacid Aquivion® PFSA as an efficient catalyst for the gas phase dehydration of ethanol to ethylene in mild conditions. *Appl. Catal. Gen.* **597**, (2020).

128. Styskalik, A., Vykoukal, V., Fusaro, L., Aprile, C. & Debecker, D. P. Mildly acidic aluminosilicate catalysts for stable performance in ethanol dehydration. *Appl. Catal. B Environ.* **271**, (2020).

129. Eagan, N. M., Kumbhalkar, M. D., Buchanan, J. S., Dumesic, J. A. & Huber, G. W. Chemistries and processes for the conversion of ethanol into middle-distillate fuels. *Nat. Rev. Chem.* **3**, 223–249 (2019).

130. Jonathan, A., Tomashek, E. G., Lanci, M. P., Dumesic, J. A. & Huber, G. W. Reaction kinetics study of ethylene oligomerization into linear olefins over carbon-supported cobalt catalysts. *J. Catal.* **404**, 954–963 (2021).

131. Kwon, M. H. *et al.* One-pot cascade ethylene oligomerization using Ni/Siral-30 and H-ZSM-5 catalysts. *Appl. Catal. Gen.* **572**, 226–231 (2019).

132. Mohamed, H. O., Abed, O., Zambrano, N., Castaño, P. & Hita, I. A Zeolite-Based Cascade System to Produce Jet Fuel from Ethylene Oligomerization. *Ind. Eng. Chem. Res.* **61**, 15880–15892 (2022).

133. Moon, S., Chae, H. J. & Park, M. B. Oligomerization of light olefins over ZSM-5 and beta zeolite catalysts by modifying textural properties. *Appl. Catal. Gen.* **553**, 15–23 (2018).

134. Lee, M. *et al.* Ni/SIRAL-30 as a heterogeneous catalyst for ethylene oligomerization. *Appl. Catal. Gen.* **562**, 87–93 (2018).

135. Martínez Gómez-Aldaraví, A., Paris, C., Moliner, M. & Martínez, C. Design of bi-functional Ni-zeolites for ethylene oligomerization: Controlling Ni speciation and zeolite properties by one-pot and post-synthetic Ni incorporation. *J. Catal.* **426**, 140–152 (2023).

136. Attanatho, L. *et al.* Jet fuel range hydrocarbon synthesis through ethylene oligomerization over platelet Ni-AlSBA-15 catalyst. *SN Appl. Sci.* **2**, (2020).

137. Panpian, P. *et al.* Production of bio-jet fuel through ethylene oligomerization using NiAlKIT-6 as a highly efficient catalyst. *Fuel* **287**, (2021).

138. Gagliardi, A. *et al.* Ethanol to gasoline and sustainable aviation fuel precursors: an innovative cascade strategy over Zr-based multifunctional catalysts in the gas phase. *Appl. Catal. B Environ. Energy* **349**, 123865 (2024).